26. GEOCHEMISTRY OF BASALTS: DEEP SEA DRILLING PROJECT SITES 482, 483, AND 485 NEAR THE TAMAYO FRACTURE ZONE, GULF OF CALIFORNIA[1]

M. F. J. Flower, Department of Geological Sciences, University of Illinois, Chicago, Illinois
R. G. Pritchard, Institut für Mineralogie der Ruhr-Universität, 463 Bochum-Querenburg, Federal Republic of Germany, and Philips GmbH, 3500 Kassel, Miramstrasse 87, Federal Republic of Germany
H.-U. Schmincke, Institut für Mineralogie der Ruhr-Universität, 463 Bochum-Querenburg, Federal Republic of Germany
and
Paul T. Robinson, Department of Geology, Dalhousie University, Halifax, Nova Scotia B3H 3J5, Canada

INTRODUCTION

Recent investigations of the southern Gulf of California (22°N) on Leg 65 of the Deep Sea Drilling Project (DSDP) (Fig. 1) allow important comparisons with drilled sections of ocean crust formed at different spreading rates. During Leg 65 the *Glomar Challenger* drilled seven basement holes at sites forming a transect across the ridge axis near the Tamayo Fracture Zone (Fig. 1). An additional site was drilled on the fracture zone itself, where a small magnetic "diapir" was located. Together with the material from Site 474 (drilled during Leg 64) the cores recovered at these sites are representative of the upper basaltic and sedimentary crust formed since the initial opening of the Gulf. The pattern of magmatic accretion at the ridge axis is conditioned by the moderate to high rate of spreading (~6 cm/y.) and comparatively high sedimentation rates that now characterize the Gulf of California. In terms of spreading rate, this region is intermediate between the "superfast" East Pacific Rise axis to the south (up to 17 cm/y.) and the slow-spreading Mid-Atlantic Ridge (2–4 cm/y.) both of which have been extensively studied by dredging and drilling.

In this chapter, we present data on major and trace elements for drilled basaltic rocks from the Tamayo transect. The samples were taken during shipboard investigation of the core and are representative of the igneous rocks encountered at each site.

CRUSTAL CONSTRUCTION IN THE GULF OF CALIFORNIA

The Gulf of California represents an early stage in the formation of an ocean basin and includes within its confines an active accretion zone, numerous transform fractures, and passive continental margins (Fig. 1). Spreading began in the Gulf about 3.5 m.y. ago, and today reflects a distinct transition in the spreading styles observed along the East Pacific Rise. South of the Tamayo Fracture Zone the rise shows comparatively simple dilation. To the north, strike-slip motion is increasingly dominant as transform fractures become more common.

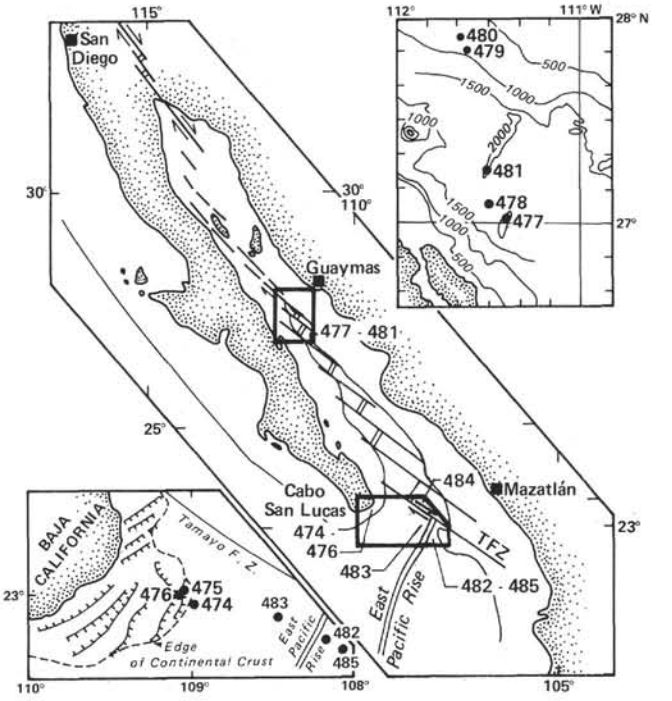

Figure 1. Map of the Gulf of California, showing areas studied on DSDP Legs 64 and 65. Note change from a dilational regime to a dominantly strike-slip regime at the Tamayo Fracture Zone (TFZ).

The southern part of the Gulf of California has been studied in considerable detail by a variety of techniques. The Leg 65 transect across the ridge axis spans most of its temporal evolution, while the "RITA" Project used submersibles to obtain morphologic, petrologic, and geochemical data for the ridge axis at 21°N (CYAMEX, in press) and along the Tamayo Fracture Zone (Kastens et al., 1979). Results of the "ROSE" experiment (e.g., Reid et al., 1977) yielded evidence for intermittent melt zones beneath the ridge axis. Seismic reflection profiling across the axis at 21–23°N (Lewis, 1979) suggests that accretion at contiguous ridge segments is episodic and may reflect flow of magma along the axis.

[1] Lewis, B. T. R., Robinson, P., et al., *Init. Repts. DSDP*, 65: Washington (U.S. Govt. Printing Office).

Studies of the Mid-Atlantic Ridge suggest that crustal accretion at slow-spreading axes is also strongly episodic and generally accompanied by tectonic disruption. The resulting crustal structure is apparently composed of imbricated lenses with little lateral continuity. Seafloor topography in the Gulf of California appears to consist of linear basalt ridges, parallel to the main axis, separated by broad flat-floored valleys. The ridges appear to comprise pillow basalt complexes, while the valleys are floored (or partially filled by) thick massive flows (Francheteau et al., 1979). There is little evidence of tectonic disturbance. The ridges may represent waning stages of a constructive cycle, while the massive units appear to represent earlier, more prolific phases of such cycles. The crustal sections revealed by drilling show an analogous pattern to that reported from submersible studies. At the deepest site, pillow lavas interlayered with thin massive flows are found in the lower levels of the section, but the upper levels consist of thick massive units of more magnesian character.

The general characteristics of crust generated at the mouth of the Gulf of California are depicted in Figure 2 for the Leg 65 sections. Sedimentation rates were lower at Site 483 west of the ridge axis than at the other sites (Rangin, this volume). Thus an equivalent depth of basement penetration at this site corresponds to a more extensive igneous section than at the other sites. The lower sections at Site 483 reveal interlayered pillows and thin massive flows. This type of sequence was not encountered at Sites 482 and 485, where only thick massive units were observed.

Excellent intrasite correlation was established at Sites 482 and 483, reflecting lithologic and chemical continuity of emplacement units over distances of at least 2,000 meters. No evidence for tectonic disturbance of the crust is apparent.

SAMPLING AND ANALYTICAL TECHNIQUES

The shipboard studies established criteria for the lithologic subdivision of the basalts recovered. Petrography, frequency of chill margins, and sedimentary intercalations in the drilled sections allowed inference of "cooling unit" divisions (not synonymous with "eruptive" units) which range from single pillows a few centimeters thick to massive units some tens of meters thick. The cooling units identified are summarized and related to lithologic units in Appendixes A and B. The cooling units are taken as a basic reference for integrating chemical and other data since it may be assumed that the properties of any given unit share a common origin. Lithologic "subunits" were defined in some cases to allow for unrecovered cooling unit boundaries.

In general, glass cooling selvedges are associated with pillows and thin massive flows. Most of the glass samples examined were from the lower parts of Holes 483 and 483B, although a small amount was sampled from Holes 482B, D, and F. Glass was not observed at Sites 484 and 485. However, aphyric, nonpillowed basalt units are common at all sites and may be considered equivalent to liquid compositions. Thus, basalt liquid-fraction compositions may be studied at all of the sites and compared with the compositions of phyric basalts from the same sites. Data for mineral compositions (Viereck, personal communication) indicate that phenocrysts mostly represent equilibrium assemblages grown *in situ* rather than accumulated phases from previous, or spatially separated, crystallization episodes. However, there is evidence for some phenocryst accumulation and resorption.

Major element concentrations were determined by X-ray fluorescence on samples prepared as glass beads. Lithium tetraborate and metaborate (rock to flux ratio 1:4) were used for fusion, and analyses were made using a Philips PW 1450 X-ray fluorescence spectrometer. Analysis for Fe^{2+} was conducted by digesting samples in hydrofluoric acid and silver perchlorate solution followed by potentiometric titration of excess perchlorate with standard potassium bromide solution. H_2O was determined by ignition in a dry inert gas atmosphere followed by coulometric titration of the effluent gas in barium perchlorate solution. Samples 482C-12-1, 92–118; 483B-8-3, 2–20; 483B-28-1, 42–59; and 485A-25-1, 117–143 were analyzed as interlaboratory comparisons; data are given in Table 1 with analytical statistics.

MAJOR ELEMENT VARIATION

The complete data set comprises 187 analyses of basalt sampled from Sites 482, 483, and 485. The major element analyses are given in Table 2 and averaged by chemical type in Table 3, while the trace elements are given in Table 4 and their ratios in Table 5. Most samples are from massive or pillowed flow units; they are fine grained with holocrystalline to intersertal textures and range from moderately phyric to aphyric. Glass selvedges associated with thin flows at Site 482 and with pillow lavas at Site 483 were sampled and analyzed using an electron microprobe. These data are given by Flower and O'Hearn (this volume) with additional whole-rock analyses. Together, the data are used to study compositional variations in the magmatic liquid fraction and the total eruptive magma (liquid plus any crystalline fraction) during the formation of crust at these localities. Following preliminary shipboard studies, we defined "chemical types" that correspond to distinct compositional-stratigraphic groupings of the data. These form a basis for interpreting petrogenetic processes.

Slight to moderate degrees of alteration were encountered in the core, as reflected by the presence of smectite—and in rare cases, talc—the latter indicating moderately high temperatures. However, altered zones were carefully avoided in sampling for this study. "Fresh" rock analyses (i.e., not significantly leached of Ca^{2+} and Mg^{2+}) were corrected for interstitial and vesicular calcite by removing CO_2-equivalent CaO and normalizing to dry weight. Using corrected data sets for each site, the chemical types were established graphically in relation to the stratigraphic and lithologic associations recorded on shipboard. With few exceptions, the chemical types defined on shipboard remain unchanged in light of the expanded data sets obtained in this study. The stratigraphic extent of lavas composing a single chemical type often correspond to rock sequences built up during a single eruption or eruptive phase. Chemical types thus appear to be a useful indicator of the chronologic patterns of fractionation.

Previous studies of oceanic basement (e.g., Flower et al., 1977; Byerly and Wright, 1978; Flower and Robinson, 1981a and b; Bryan et al., 1978) suggest that compositional differences between chemical types may reflect the effects of both deep-seated and comparatively shallow-level fractionation. Such processes would be expected to include fractional crystallization, as constrained by polybaric phase equilibria and mixing of magma batches at various stages of the liquids' evolution. Although we assume that lavas belonging to a single chemical type reflect a common fractionation and eruptive history, we focus attention on variations both within and between each type. The average composi-

tions of the chemical types encountered at Leg 65 sites are given in Table 3, and the petrography of the core material is summarized in Appendix B in relation to chemical types and lithologic units.

Compositional variations are depicted according to chemical type in plots of weight percent FeO* (i.e., total Fe oxide), Al_2O_3, and TiO_2 versus MgO. This type of oxide variation diagram permits simple graphical distinction between liquid variation trends resulting from fractional crystallization and contrasting trends resulting from the effects of phenocryst accumulation and, possibly, alteration.

Whole-Rock Variation, Site 482

The Site 482 chemical types (A–H inclusive) are best represented at Hole 482B and less completely at Holes 482C, D, and F. All but one of the cooling units identified at this site are massive and probably eruptive, while the chemical types may include more than a single cooling unit. The chemical variation (Fig. 3) appears to reflect a combination of liquid phase variation and phenocryst accumulation processes. Chemical Type A is represented by the uppermost basalt unit in Holes 482B, C, and D (Lithologic Unit 1), an aphyric flow extending at least 1000 meters laterally. Chemical Type E is slightly more Al_2O_3-rich, but otherwise very similar to Type A, and they are grouped together in the diagrams. Chemical Types B and F are indistinguishable in terms of major elements, but Type F is characterized by a notably higher Ni content and a lower Zr/Ni ratio than B (Table 5). Chemical Type F is absent from Hole 482C but separates Types A and B in Hole 482B. Both Types B and F are distinguished from Type A by lower TiO_2 and FeO* and higher Al_2O_3 for equivalent MgO content (Fig. 3). Chemical Type D is represented at the base of Hole 482B (only) by phyric Lithologic Units 7 and 8 and also by the intercalated Unit 5. The plagioclase-phyric lithology and chemical variation of Chemical Type D suggest a derivation from a low-TiO_2 magma (Chemical Type A?) involving some accumulation of plagioclase (Fig. 3). In general, there is excellent correlation between the holes at this site for Chemical Types A and B and, between Holes 482B and D for Type F. It is assumed that Type D would be encountered by deeper penetration in Holes 482C and D. Least-squares analysis of the major element variation within and between the Site 482 chemical types (Table 6) suggests that two or more stages of fractionation were involved, both before and after segregation of the magma into the batches now represented by chemical types.

Whole-Rock Variation, Site 483

The patterns of whole-rock variation observed at Site 483 (Fig. 4) show that the chemical types encountered are related to the inferred emplacement mode, namely massive versus pillowed cooling units. On the basis of lithologic and magnetic stratigraphy (Day, this volume), drilling rate, and geophysical logging (see site summaries, and Salisbury, this volume), we have established an excellent cross-hole correlation between cooling units and chemical types. The upper four basalt units show a simple cross-hole correspondence matched by thick sedimentary interlayers. Lithologic Unit 5 at Hole 483 (Chemical Type E) is equivalent to a nonrecovered basalt interval intercalated with the sediment in Hole 483B. Likewise, a nonrecovered basalt interval recorded by logging in Hole 483 corresponds to a pillow sequence (Chemical Type I) in Hole 483B. The cross-hole correlation continues down-section, with several massive flow units of Chemical Type H traced between each hole. The resultant stratigraphic synthesis allows complete identification of the massive units at this site.

In summary, the crustal structure at Site 483 may be divided into two parts:

1) Chemical Types A–D (Lithologic Units 1–4) make up the "upper" massive units, separated by thick sediment intercalations. These units are comparatively rich in MgO (7.2–10.0 wt.%), CaO, and Al_2O_3, and low in TiO_2, FeO, and P_2O_5.

2) Chemical types E–M (Lithologic Units 5–9) make up an intercalated series of pillow and thin massive basalt sequences. These have MgO contents of 7.0–7.4 wt.% and distinctly higher TiO_2 and FeO* values than do the "upper" massive units.

Several discrete massive units belonging to Chemical Types H and K show similar variation patterns (Fig. 4). These units are notably more fractionated than the "upper" massive units. These groups depart compositionally from the overall variation trend represented by the whole-rock data and, more particularly, the glass data (Flower and O'Hearn, this volume). Least-squares analysis of the intraunit variation suggests that complex phenocryst redistribution processes involving the accumulation of plagioclase took place in some cases.

The pillow units (Chemical Types F, I, J, L, and M) are generally more phyric than the massive units. While showing similar individual trends, these units reflect considerably more diffuse variation than the massive units. Least-squares tests indicate that simple phenocryst removal during cotectic fractionation is insufficient to explain the variations observed between and within chemical types (Table 6). Chemical Types D, B, K, and H appear to require some accumulation of plagioclase concomitant with the removal of olivine and clinopyroxene to satisfy internal mass balance requirements. This appears to be a common characteristic of the massive eruptions but is not supported by the sparsely phyric or aphyric petrography of these units.

Whole-Rock Variation, Site 485

Shipboard analysis of samples from Site 485 was not completed on board. Thus chemical types were not previously defined for this site. In this study, chemical types were defined which in several cases correspond to single massive units. For the eight basaltic units drilled at Site 485, chemical types were assigned as follows: 1: A, B, C, and E; 2: Z?; 3 (not analyzed); 4: H; 5: I; 6: J; 7: K; and 8: L. Each lithologic unit probably represents a single emplacement event. However, in some cases (e.g., Units 1 and 5 especially) each may comprise several intrusive and/or extrusive subunits. This is reflected by

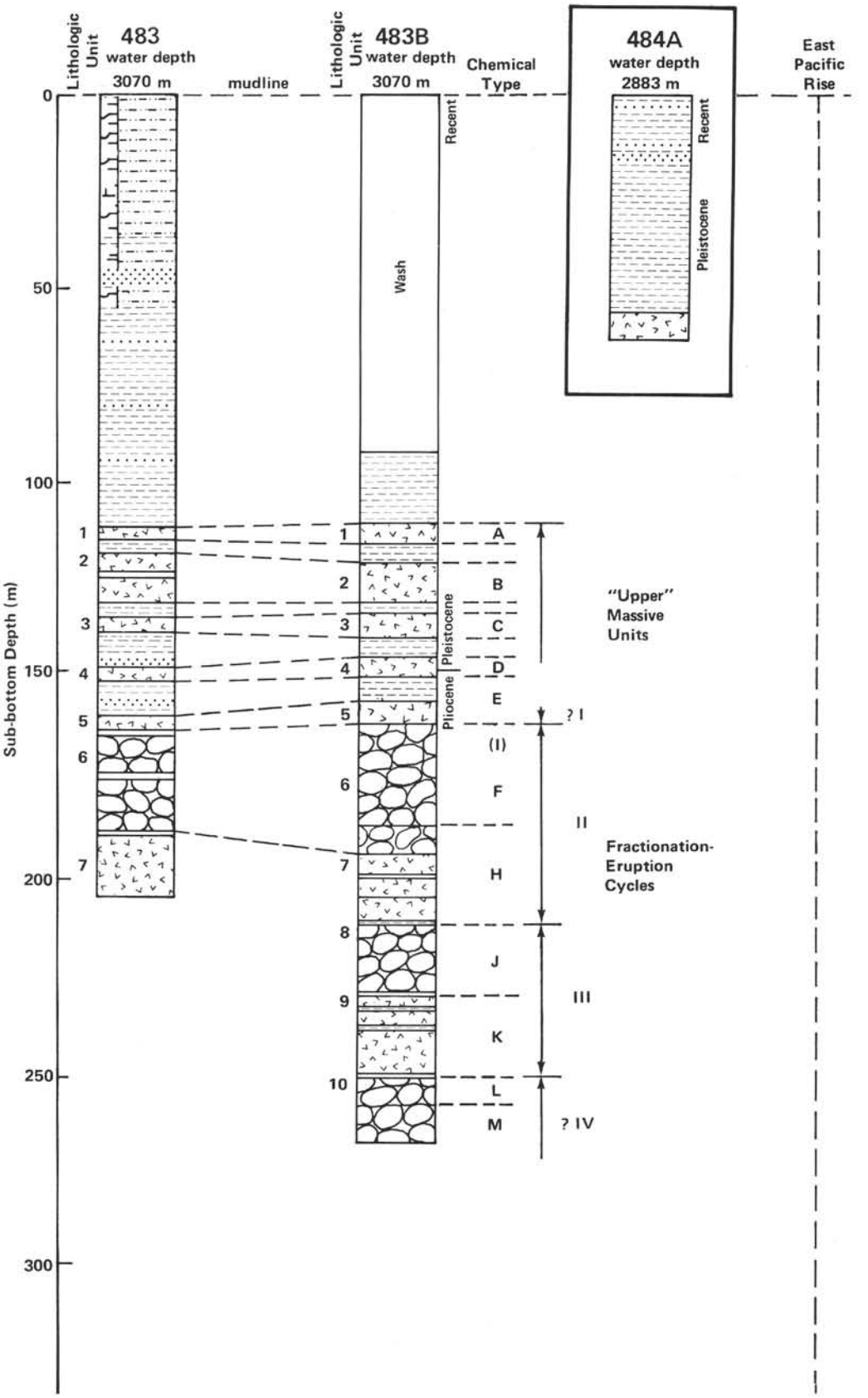

Figure 2. Sections drilled during Leg 65. Chemical types identified in this study and between-hole correlations at Sites 482 and 483 are indicated. No samples from Site 484 were analyzed. (Water depths shown in meters at the top of each section.)

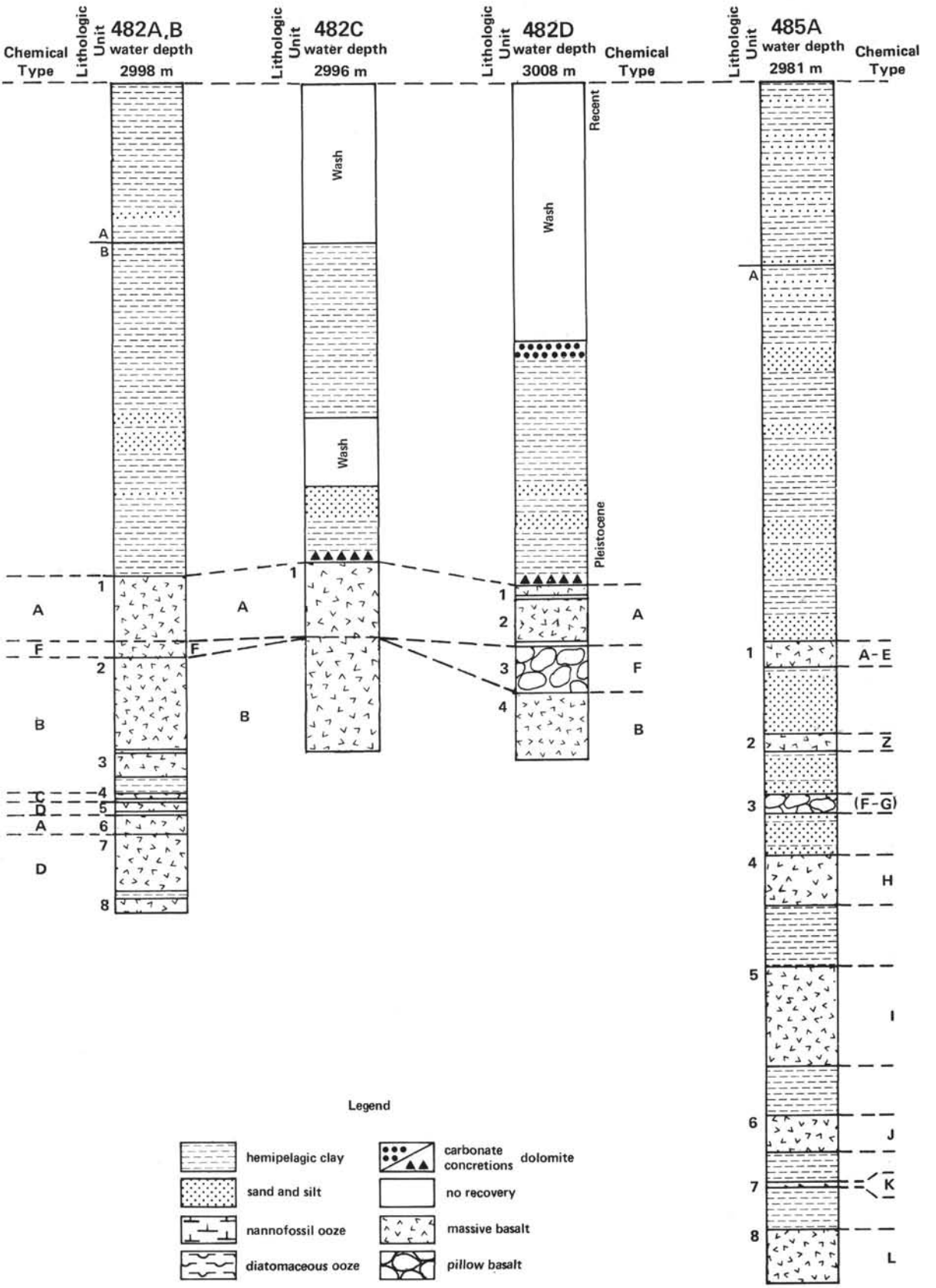

Figure 2. (Continued).

Table 1. Interlaboratory comparison of analyses.

Oxide	ALB[a]	BIR[a]	BOC[a]	BRE[a]	ICL[a]	Mean	2σ
Sample 482C-12-1, 91-118 cm							
SiO_2	50.21	50.11	50.30	50.24	50.29	50.22	0.07
Al_2O_3	14.74	14.94	14.60	14.78	14.64	14.74	0.13
Fe_2O_3*	11.12	11.11	11.00	11.29	11.02	11.11	0.11
MgO	7.78	7.98	7.81	7.88	7.79	7.85	0.09
CaO	11.78	12.08	12.40	12.26	12.10	12.13	0.23
Na_2O	2.47	2.27	2.47	1.96	2.38	2.31	0.21
K_2O	0.06	0.06	0.05	0.07	0.06	0.06	<0.01
TiO_2	1.23	1.30	1.27	1.29	1.26	1.27	0.03
P_2O_5	0.10	0.11	0.11	0.15	0.12	0.12	0.02
MnO	0.16	0.15	0.18	0.18	0.16	0.17	0.01
Total	99.65	100.14	100.20	100.10	99.82	99.98	
H_2O^+	0.90	nd	0.93	nd	nd		
CO_2	nd	nd	0.13	nd	nd		
Sample 483B-8-3, 2-20 cm							
Oxide	ALB	BIR	BOC	BRE	ICL	Mean	2σ
SiO_2	48.59	48.90	48.50	48.33	48.80	48.63	0.23
Al_2O_3	16.66	16.42	16.40	16.52	16.58	16.52	0.18
Fe_2O_3*	10.06	9.64	9.57	9.86	9.84	9.79	0.19
MgO	9.05	9.76	9.29	9.35	9.26	9.34	0.26
CaO	12.89	12.05	12.20	12.28	12.21	12.12	0.15
Na_2O	2.27	2.14	2.20	2.27	2.13	2.20	0.07
K_2O	0.04	0.05	0.04	0.04	0.05	0.04	<0.01
TiO_2	1.01	1.07	1.06	1.07	1.06	1.05	0.03
P_2O_5	0.07	0.08	0.08	0.12	0.09	0.09	<0.02
MnO	0.15	0.15	0.16	0.16	0.17	0.16	<0.01
Total	99.79	100.26	99.49	100.00	100.19	99.95	
H_2O^+	1.94	nd	1.80	nd	nd		
CO_2	nd	nd	0.35	nd	nd		
Sample 483B-28-1, 42-59 cm							
Oxide	ALB	BIR	BOC	BRE	ICL	Mean	2σ
SiO_2	49.63	49.63	49.70	49.58	49.51	49.61	0.07
Al_2O_3	14.35	14.48	14.10	14.17	14.17	14.26	0.15
Fe_2O_3*	12.40	12.17	12.00	12.36	12.03	12.18	0.19
MgO	7.56	7.63	7.72	7.73	7.69	7.67	0.07
CaO	11.19	11.46	11.70	11.66	11.45	11.49	0.20
Na_2O	2.72	2.56	2.66	2.23	2.55	2.54	0.19
K_2O	0.10	0.10	0.09	0.10	0.10	0.10	<0.01
TiO_2	1.72	1.92	1.77	1.81	1.76	1.80	0.08
P_2O_5	0.15	0.15	0.15	0.19	0.15	0.16	0.02
MnO	0.18	0.16	0.19	0.18	0.22	0.19	0.02
Total	100.00	100.26	100.10	100.01	99.63	99.99	
H_2O^+	1.18	nd	1.25	nd	nd		
CO_2	nd	nd	0.19	nd	nd		
Sample 485A-25-1, 117-143 cm							
Oxide	ALB	BIR	BOC	BRE	ICL	Mean	2σ
SiO_2	49.69	49.34	49.80	49.09	49.20	49.44	0.32
Al_2O_3	14.61	14.80	14.70	14.43	14.53	14.60	0.14
Fe_2O_3*	12.44	12.61	12.60	12.88	12.60	12.63	0.16
MgO	7.18	7.20	7.25	7.11	7.22	7.19	0.05
CaO	10.71	11.03	11.20	11.20	11.07	11.05	0.20
Na_2O	2.65	2.49	2.61	2.50	2.50	2.55	0.07
K_2O	0.09	0.08	0.08	0.08	0.08	0.08	<0.01
TiO_2	2.07	2.34	2.13	2.15	2.11	2.16	0.10
P_2O_5	0.19	0.21	0.20	0.21	0.21	0.20	<0.01
Total	99.83	100.34	100.80	99.85	99.74	100.11	
H_2O^+	1.05	nd	1.02	nd	nd		
CO_2	nd	nd	0.15	nd	nd		

[a] BOC-Ruhr-Univ., Bochum; BIR = Univ. of Birmingham; ALB = Univ. of New Mexico, Albuquerque; BRE = CNEXO, Brest; ICL = Imperial College, London.

significant internal chemical diversity. We infer intrusive origins where the basalt groundmass textures are particularly coarse grained. Intrusive contacts were only observed, however, for Unit 5.

In general, and in contrast to Site 483, the chemical variation within and between the Site 485 chemical types (Fig. 5) appears consistent with a single parental magma type (cf. Site 483). However, internal variation within, for example, Type I (Unit 5) indicates a complex fractionation history prior to or during emplacement. Intraunit variation is in most cases attributed to fractional crystallization and possibly to some minor flow differentiation during emplacement. The massive units include a total of 28 lithologic subunits defined during shipboard core description.

Lithologic Unit 1 comprises Cooling Units 1-5 (A-E in Fig. 5), which correspond to at least three internal variation trends: A, E, and B-C. The upper part of Unit 1 (Type A) shows a comparatively high MgO content. The most magnesian sample analyzed is unaltered, shows little evidence of olivine accumulation, and appears to represent a liquid composition. The internal trends are similar to the massive unit trends at Site 483 (Fig. 4) and in some cases (see Table 6) require accumulation of plagioclase concomitant with mafic phase fractionation (Table 6). The parent batches may belong to one or several fractionation trends of a more deep-seated origin. Lithologic Unit 2 is represented by one analysis which is compositionally distinct from Chemical Types A-E. Lithologic Unit 4, in contrast, is comparatively uniform in composition (Type H in Fig. 5). Lithologic Unit 5 is similar to Unit 1 and shows considerable internal variation. This unit, identified on shipboard as a single cooling unit (9), can be subdivided chemically into at least five stratigraphically contiguous units, each corresponding to one or several lithologic subunit divisions (i.e., Subunits 9/16-9/22). Such complex variation suggests that the emplacement of this unit may have involved a combination of extrusion and late-stage intrusive events. Least-squares solutions for the internal variation indicate that similar phenocryst redistribution patterns affected several compositionally distinct parent batches. As for Site 483 Chemical Type D, the very sparsely phyric character of Unit 5 does not suggest plagioclase accumulation, although this appears to be required by the least-squares solutions (Table 6). A more complex origin is thus indicated. Lithologic Units 6, 7, and 8 consist of sparsely- to moderately-phyric basalt and each represents a single cooling unit. The data are insufficient to categorize Unit 7 (the single analysis, Type K in Fig. 5, is strongly indicative of plagioclase accumulation), but Units 6 and 8 (J and L in Fig. 5) reflect little internal variation compared to Units 5 and 1. They are also indistinguishable from each other, but separated stratigraphically by the distinctive Type K.

Of the eight major basalt units cored at Site 485, at least two (1 and 5) show complex internal variation patterns. These are indicative of discrete fractionation events superimposed on one or more compositional trends of deeper-seated origin.

TRACE ELEMENT VARIATION

The trace elements Cr, Ni, Cu, Zn, Rb, Sr, Y, Zr, and Nb were analyzed for all 187 samples (Tables 4 and 5)

Table 2. Major element compositions of fresh basalts from DSDP Sites 482, 483, and 485[a].

Sample (interval in cm)	SiO_2	Al_2O_3	FeO*	MgO	CaO	Na_2O	K_2O	TiO_2	P_2O_5	MnO
					(wt.%)					
Hole 482B										
13-1, 99–104	50.73	14.36	10.39	8.10	11.53	2.57	0.06	1.80	0.15	0.19
14-1, 91–94	50.18	15.40	10.10	7.86	11.83	2.45	0.07	1.46	0.11	0.18
14-1, 132–137	50.27	15.09	10.05	7.73	12.15	2.62	0.05	1.39	0.12	0.19
14-3, 2–6	50.28	15.01	10.03	8.04	11.99	2.37	0.07	1.42	0.11	0.18
14-4, 16–20	50.21	14.85	10.22	8.00	12.14	2.45	0.07	1.43	0.12	0.19
15-1, 12–16	50.49	15.48	10.15	7.96	11.44	2.51	0.07	1.48	0.11	0.18
16-4, 100–104	51.04	14.65	10.00	8.13	11.96	2.29	0.06	1.28	0.11	0.17
20-1, 27–30	50.20	15.33	10.09	7.33	12.02	2.56	0.06	1.59	0.13	0.20
20-3, 144–147	50.49	14.69	10.32	7.45	12.33	2.50	0.03	1.51	0.13	0.19
21-2, 19–23	50.78	14.72	10.28	7.46	12.06	2.49	0.03	1.51	0.13	0.18
21-3, 58–63	50.07	15.60	9.89	7.26	12.15	2.71	0.04	1.60	0.15	0.19
22-2, 67–72	50.32	15.52	9.70	7.31	12.22	2.72	0.03	1.56	0.14	0.19
22-2, 130–136	50.08	15.90	9.58	7.06	12.35	2.77	0.03	1.58	0.14	0.17
22-3, 103–107	49.98	15.39	9.69	7.84	12.37	2.52	0.04	1.50	0.14	0.18
22-4, 97–102	49.96	15.93	9.64	7.49	12.00	2.70	0.06	1.57	0.15	0.17
24-3, 110–115	50.57	14.21	10.58	7.53	11.67	2.78	0.06	1.87	0.16	0.17
Hole 482C										
10-1, 0–4	50.03	15.59	9.93	8.51	10.31	2.64	0.10	1.92	0.15	0.17
10-1, 9–12	50.05	14.49	10.34	7.93	12.10	2.33	0.11	1.83	0.17	0.24
10-1, 12–16	50.00	14.70	10.01	8.04	11.90	2.58	0.06	1.84	0.17	0.23
10-3, 11–14	50.58	14.42	10.20	8.15	11.53	2.62	0.07	1.73	0.15	0.18
11-3, 65–69	50.33	14.39	10.40	7.80	11.92	2.63	0.08	1.76	0.16	0.18
12-1, 92–118	50.66	14.75	9.98	7.88	12.30	2.49	0.05	1.28	0.11	0.18
13-1, 10–15	50.54	15.41	9.20	8.28	11.77	2.39	0.04	1.32	0.11	0.15
14-1, 13–18	50.81	14.47	10.11	8.06	12.13	2.42	0.05	1.32	0.11	0.18
15-1, 114–118	50.78	14.89	9.98	8.72	10.97	2.54	0.08	1.35	0.12	0.18
Hole 482D										
8-1, 24–29	50.52	14.80	10.25	8.04	11.29	2.46	0.06	1.80	0.16	0.22
8-1, 65–72	50.57	14.93	9.81	7.25	12.04	2.50	0.00	1.80	0.17	0.28
10-1, 106–109	50.49	14.91	10.04	8.13	11.89	2.47	0.04	1.43	0.12	0.18
10-1, 111–114	50.36	15.11	9.53	8.02	11.54	2.81	0.07	1.81	0.17	0.16
10-2, 70–72	50.33	14.55	10.70	7.68	11.69	2.51	0.05	1.80	0.15	0.19
10-2, 128–130	50.47	14.64	10.16	7.72	11.76	2.56	0.05	1.88	0.17	0.18
10-3, 25–27	50.71	14.14	10.73	7.85	11.00	2.74	0.06	2.02	0.17	0.17
10-3, 93–97	50.34	15.04	10.05	8.23	11.84	2.45	0.06	1.44	0.11	0.18
12-1, 28–32	50.16	14.92	10.07	8.12	12.00	2.47	0.07	1.41	0.12	0.18
12-3, 27–31	50.16	14.82	10.25	8.24	12.22	2.32	0.03	1.31	0.11	0.18
13-1, 49–51	50.84	15.37	9.34	8.32	11.37	2.68	0.04	1.37	0.11	0.15
13-1, 98–101	50.36	14.74	10.02	8.22	12.38	2.32	0.03	1.30	0.11	0.19
13-1, 128–134	50.86	14.75	9.93	8.28	11.75	2.43	0.05	1.34	0.11	0.18
Hole 482F										
5-1, 133–139	50.57	14.34	11.35	6.84	10.97	2.85	0.11	2.14	0.20	0.19
11-1, 125–128	50.39	14.91	10.02	8.28	11.86	2.45	0.05	1.43	0.11	0.18
Hole 483										
14-1, 58–68	50.88	15.34	9.27	8.03	11.89	2.66	0.06	1.23	0.09	0.17
15-1, 93–97	50.89	15.24	8.89	7.77	12.71	2.59	0.06	1.24	0.09	0.16
16-2, 64–70	50.77	14.71	10.02	7.90	11.81	2.75	0.07	1.41	0.10	0.18
16-2, 99–100	50.55	14.84	9.71	7.89	12.10	2.75	0.07	1.42	0.11	0.16
16-3, 2–6	50.68	15.04	9.49	8.04	11.98	2.77	0.07	1.34	0.10	0.17
17-2, 13–17	50.00	17.07	7.87	8.82	12.54	2.22	0.03	1.00	0.07	0.15
17-2, 17–21	49.56	16.86	8.25	9.76	12.09	2.09	0.03	0.90	0.06	0.17
18-4, 131–134	50.90	16.41	8.45	7.41	10.95	3.18	0.16	1.84	0.18	0.15
21-1, 49–55	50.36	14.64	10.97	7.25	11.50	2.61	0.09	1.92	0.17	0.22
21-1, 57–61	50.42	14.93	10.81	7.12	11.54	2.49	0.12	1.90	0.17	0.21
21-3, 6–9	49.96	14.80	10.84	7.44	11.42	2.73	0.09	1.96	0.18	0.24
22-2, 68–72	50.04	15.48	9.95	7.20	12.31	2.58	0.08	1.67	0.15	0.21
22-2, 74–77	50.26	15.27	10.13	7.43	12.03	2.48	0.08	1.68	0.14	0.20
22-2, 85–88	50.47	15.19	10.20	7.38	11.95	2.44	0.11	1.66	0.14	0.18
22-2, 88–93	49.97	16.11	9.83	6.64	12.37	2.57	0.07	1.71	0.16	0.20
22-2, 94–99	50.16	15.92	9.96	6.94	11.95	2.60	0.09	1.70	0.14	0.20
23-1, 10–16	49.76	15.90	10.08	6.91	12.28	2.52	0.05	1.74	0.16	0.20
24-1, 52–57	49.76	15.17	10.94	6.96	10.79	3.06	0.08	2.35	0.22	0.17
24-2, 35–40	50.54	14.39	11.33	6.82	11.11	2.73	0.11	2.14	0.21	0.19
25-2, 61–66	50.53	14.06	11.59	7.16	10.97	2.69	0.10	2.13	0.19	0.19
26-1, 59–63	49.23	14.66	11.47	7.28	11.52	2.64	0.07	2.14	0.21	0.22
26-2, 40–44	49.28	14.81	11.39	7.20	11.61	2.64	0.06	2.11	0.20	0.21
26-3, 124–130	50.38	14.21	11.43	7.07	11.03	2.81	0.07	2.21	0.20	0.18
Hole 483B										
4-1, 26–30	50.77	15.00	9.24	8.24	12.20	2.63	0.07	1.24	0.09	0.15
7-1, 7–12	50.44	14.59	10.15	7.68	12.30	2.73	0.06	1.42	0.10	0.18
7-1, 26–31	50.37	14.54	10.16	7.94	12.33	2.66	0.05	1.36	0.10	0.18
7-2, 56–61	50.66	14.54	9.91	7.98	12.19	2.67	0.05	1.37	0.10	0.18
7-3, 2–6	50.80	14.76	10.08	7.41	12.16	2.75	0.05	1.38	0.09	0.17
8-1, 29–35	50.26	17.42	8.00	7.76	12.63	2.40	0.04	1.01	0.07	0.16
8-1, 55–61	49.39	16.43	8.53	9.94	12.30	2.13	0.03	0.98	0.07	0.16
8-1, 120–126	49.54	16.83	8.14	8.91	12.81	2.28	0.03	1.00	0.07	0.16
8-2, 121–126	50.08	16.51	8.26	8.86	12.15	2.49	0.05	1.10	0.08	0.16
8-7, 2–20	49.32	16.72	8.75	9.44	11.92	2.24	0.04	1.07	0.08	0.16
12-1, 92–95	49.75	15.60	10.30	7.18	12.00	2.60	0.06	1.57	0.13	0.20
13-1, 38–44	50.49	14.65	10.95	7.07	11.54	2.61	0.08	1.89	0.17	0.19
13-1, 60–64	50.18	14.65	10.83	7.21	11.58	2.76	0.08	1.93	0.17	0.20
13-1, 60–64	50.00	15.03	10.61	7.12	11.74	2.70	0.07	1.95	0.18	0.20
13-1, 66–67	50.03	14.83	11.07	7.16	11.52	2.64	0.06	1.95	0.18	0.19
13-1, 66–67	50.20	14.68	11.20	6.98	11.57	2.62	0.09	1.94	0.18	0.20
13-1, 74–79	50.36	14.66	10.98	7.07	11.67	2.54	0.10	1.92	0.17	0.19
13-1, 92–98	50.26	14.82	10.88	7.23	11.73	2.52	0.09	1.76	0.15	0.19
13-1, 108–119	50.23	14.78	11.01	6.87	11.88	2.53	0.13	1.86	0.17	0.20
13-1, 115–122	50.13	14.52	11.50	7.06	11.34	2.65	0.08	1.97	0.17	0.19
13-1, 115–122	50.01	14.99	10.71	7.18	11.66	2.76	0.06	1.89	0.18	0.18
13-1, 124–131	50.05	14.99	10.74	7.14	11.68	2.69	0.07	1.90	0.17	0.18
13-1, 124–131	50.19	14.80	10.81	7.38	11.53	2.62	0.07	1.87	0.16	0.18
13-1, 134–139	50.28	14.82	11.04	6.73	11.64	2.61	0.11	2.00	0.18	0.20
14-1, 130–133	49.99	15.13	10.65	7.10	11.91	2.59	0.08	1.78	0.17	0.21
18-1, 49–52	50.05	14.30	12.27	7.65	9.58	2.87	0.10	2.26	0.20	0.17
18-1, 103–107	50.55	14.37	11.24	7.41	10.54	2.76	0.09	2.17	0.19	0.17
18-2, 18–22	50.61	14.10	11.25	7.66	10.40	2.84	0.07	2.20	0.20	0.18

Table 2. (Continued).

Sample (interval in cm)	SiO_2	Al_2O_3	FeO*	MgO	CaO	Na_2O	K_2O	TiO_2	P_2O_5	MnO
					(wt.%)					
Hole 482B										
19-2, 17–21	50.23	14.24	11.51	6.77	11.15	2.71	0.10	2.15	0.21	0.19
19-2, 104–108	50.22	14.65	11.36	6.87	10.78	2.88	0.08	2.29	0.24	0.20
19-3, 8–12	49.75	14.88	11.01	7.01	11.14	2.94	0.11	2.19	0.22	0.21
20-1, 14–19	49.81	14.66	11.07	7.29	11.29	2.82	0.00	2.13	0.20	0.19
20-1, 94–99	49.92	14.69	11.00	7.40	11.06	2.81	0.12	2.13	0.20	0.19
20-2, 9–14	50.35	14.40	11.14	7.13	11.22	2.73	0.11	2.09	0.20	0.19
20-2, 16–21	50.41	14.11	11.55	7.16	11.13	2.68	0.10	2.08	0.20	0.20
20-2, 25–30	50.56	13.95	11.65	7.36	10.79	2.65	0.10	2.15	0.19	0.20
20-2, 37–42	50.31	14.09	11.45	7.26	11.20	2.66	0.10	2.14	0.20	0.20
20-2, 50–59	49.83	14.75	11.35	7.66	10.27	2.93	0.11	2.23	0.21	0.17
20-2, 50–59	49.77	14.42	11.56	7.62	10.74	2.79	0.10	2.19	0.20	0.19
20-2, 50–59	50.14	14.54	11.51	7.33	10.52	2.79	0.11	2.22	0.20	0.19
20-2, 142–146	49.84	14.83	10.84	7.30	11.32	2.92	0.10	2.05	0.20	0.18
21-2, 57–61	50.09	15.19	10.23	7.44	11.57	2.75	0.11	1.80	0.16	0.23
22-1, 26–32	49.97	14.91	10.59	7.31	11.77	2.73	0.12	1.81	0.16	0.22
22-2, 63–67	50.18	15.20	9.57	7.69	12.27	2.63	0.07	1.64	0.15	0.18
22-2, 77–82	50.31	14.63	10.45	7.72	11.97	2.51	0.07	1.70	0.14	0.21
23-4, 19–24	50.49	15.00	10.22	7.48	11.87	2.56	0.05	1.69	0.14	0.19
25-2, 18–20	66.93	16.30	3.61	7.12	1.65	2.40	0.07	0.63	0.20	0.03
25-2, 22–28	50.32	15.14	10.36	7.42	11.00	2.89	0.06	2.02	0.17	0.17
25-2, 39–45	49.62	14.65	11.09	7.26	11.99	2.67	0.05	1.87	0.16	0.20
26-2, 42–47	49.47	14.43	11.47	7.73	11.24	2.62	0.22	1.78	0.17	0.21
25-2, 126–137	49.83	14.54	11.10	8.05	10.96	2.68	0.14	1.75	0.16	0.19
27-1, 12–18	50.32	15.80	9.63	7.16	11.46	2.91	0.07	1.88	0.17	0.16
27-1, 114–119	50.49	14.73	10.79	7.06	11.48	2.75	0.08	1.85	0.16	0.18
27-2, 95–101	50.36	14.39	11.06	7.37	11.42	2.69	0.10	1.89	0.15	0.18
27-3, 94–98	49.97	13.79	11.45	7.58	11.65	2.78	0.09	1.93	0.16	0.19
27-4, 74–80	50.20	14.52	10.46	7.61	11.89	2.75	0.10	1.77	0.16	0.18
28-1, 42–59	50.20	14.27	10.88	7.80	11.57	2.69	0.09	1.78	0.15	0.19
28-1, 123–128	50.25	14.43	10.44	7.80	12.03	2.60	0.07	1.69	0.15	0.18
28-2, 28–32	50.26	14.40	10.36	8.00	12.04	2.53	0.07	1.65	0.15	0.18
28-3, 37–40	50.19	14.28	10.39	8.47	11.68	2.51	0.09	1.66	0.14	0.18
29-1, 10–15	49.84	14.27	10.69	8.22	11.92	2.61	0.08	1.70	0.15	0.18
29-1, 26–31	50.11	14.22	10.63	8.13	11.71	2.65	0.09	1.76	0.15	0.18
29-1, 40–45	50.17	14.54	10.80	7.53	11.68	2.67	0.06	1.77	0.15	0.19
29-1, 55–57	50.13	14.57	10.97	7.30	11.75	2.68	0.06	1.81	0.16	0.20
29-1, 57–62	51.11	15.77	9.28	7.32	10.53	3.10	0.11	1.98	0.16	0.19
29-1, 57–62	49.97	14.73	10.71	7.31	11.98	2.72	0.05	1.81	0.16	0.20
30-3, 13–16	50.17	15.04	10.38	7.54	11.56	2.67	0.08	1.79	0.17	0.23
30-3, 18–22	50.27	14.67	10.58	7.59	11.55	2.60	0.13	1.81	0.15	0.22
31-3, 20–25	50.24	15.82	9.48	7.39	11.53	2.91	0.14	1.70	0.17	0.18
32-1, 1–6	50.50	15.07	10.06	7.73	11.52	2.58	0.17	1.59	0.14	0.21
32-1, 27–31	50.09	15.54	9.47	7.65	12.21	2.63	0.10	1.59	0.14	0.18
32-1, 44–50	50.25	15.51	9.38	7.72	12.21	2.61	0.05	1.61	0.14	0.17
32-1, 90–94	50.17	15.41	9.83	7.51	11.90	2.64	0.14	1.62	0.16	0.22
32-1, 90–94	50.17	15.65	9.53	7.67	11.79	2.70	0.16	1.61	0.15	0.20
32-1, 84–88	50.12	15.70	9.39	7.62	12.08	2.64	0.11	1.60	0.14	0.23
Hole 483C										
4-4, 58–66	50.69	14.66	9.96	7.72	12.33	2.64	0.05	1.33	0.10	0.17
Hole 485A										
11-3, 57–60	49.83	18.61	9.25	5.55	10.97	3.37	0.04	1.64	0.10	0.12
11-3, 68–73	49.52	16.23	9.37	8.71	11.19	2.90	0.03	1.47	0.10	0.15
11-3, 116–121	50.02	17.03	9.36	7.04	11.46	2.94	0.03	1.50	0.09	0.13
12-1, 10–16	50.33	13.88	11.89	6.81	11.58	2.59	0.09	2.08	0.19	0.23
12-1, 76–82	50.45	13.78	12.07	6.87	11.34	2.55	0.07	2.11	0.19	0.23
12-1, 114–120	50.62	13.96	11.72	7.09	11.16	2.59	0.04	2.08	0.20	0.21
13-1, 11–18	50.62	14.46	11.54	6.71	11.34	2.47	0.08	2.01	0.18	0.23
13-1, 110–117	50.66	13.96	11.76	7.48	10.70	2.53	0.06	2.02	0.18	0.20
17-1, 77–82	49.70	15.38	12.02	7.81	8.82	2.96	0.05	2.32	0.20	0.19
23-1, 50–56	50.08	14.53	11.21	7.03	10.47	3.29	0.21	2.30	0.20	0.13
23-1, 50–56	49.43	14.94	12.32	6.99	9.30	3.41	0.30	2.27	0.20	0.10
23-1, 50–56	49.95	14.40	11.38	6.85	11.09	2.88	0.12	2.32	0.21	0.19
23-1, 148–149	50.20	14.94	11.12	7.01	11.00	2.61	0.09	2.18	0.20	0.18
23-2, 16–22	50.20	14.74	11.27	7.05	10.99	2.65	0.08	2.17	0.20	0.21
23-3, 120–125	50.16	15.04	10.69	7.03	11.02	2.93	0.07	2.23	0.20	0.19
25-1, 117–143	49.95	14.68	11.39	7.27	11.05	2.61	0.08	2.13	0.20	0.21
29-1, 2–8	49.77	14.55	11.47	7.86	10.64	2.57	0.08	2.27	0.20	0.17
29-1, 89–93	50.13	14.66	11.25	7.48	10.65	2.62	0.14	2.28	0.20	0.18
29-2, 143–148	50.20	14.78	10.80	7.25	11.60	2.69	0.05	1.97	0.18	0.19
29-3, 10–16	50.27	14.33	11.03	7.52	11.01	2.72	0.09	2.24	0.19	0.17
30-2, 96–101	50.82	13.40	11.37	7.57	11.20	2.55	0.10	2.12	0.19	0.24
30-3, 38–41	50.61	14.03	9.77	8.08	12.63	2.36	0.08	1.78	0.16	0.17
30-3, 44–49	50.71	14.68	9.22	8.14	11.96	2.68	0.06	1.81	0.15	0.16
30-4, 8–13	50.77	16.01	9.76	6.98	10.87	2.79	0.07	1.95	0.18	0.17
31-1, 62–67	50.13	14.82	9.31	8.52	12.76	2.32	0.09	1.46	0.11	0.17
31-3, 34–39	49.41	15.32	10.97	7.66	11.17	2.62	0.15	1.90	0.18	0.19
32-1, 55–61	49.37	15.11	11.26	7.98	10.51	2.87	0.13	1.97	0.20	0.20
32-2, 99–105	49.18	15.39	11.56	7.90	10.38	2.65	0.17	1.97	0.17	0.20
32-3, 47–51	49.15	14.81	11.07	8.15	10.94	2.65	0.14	1.97	0.18	0.19
32-5, 9–14	49.46	14.55	11.14	8.14	11.00	2.73	0.12	2.04	0.19	0.20
32-6, 52–57	49.71	14.43	11.77	7.65	10.63	2.64	0.16	2.21	0.19	0.21
33-1, 2–9	49.80	14.43	11.70	7.84	10.60	2.45	0.17	2.17	0.19	0.22
33-1, 74–79	49.31	14.52	11.81	7.72	10.85	2.63	0.18	2.15	0.20	0.21
33-2, 26–33	49.64	14.35	11.66	7.96	10.81	2.53	0.15	2.14	0.19	0.21
33-2, 72–78	49.86	14.40	11.80	7.82	10.53	2.47	0.17	2.18	0.19	0.20
33-2, 88–94	49.57	14.48	11.79	7.45	10.77	2.67	0.19	2.18	0.21	0.19
34-1, 86–90	50.76	14.94	10.27	7.56	11.00	2.71	0.06	1.87	0.16	0.16
34-2, 96–102	50.26	14.41	10.68	7.72	11.75	2.66	0.06	1.76	0.15	0.19
35-1, 135–142	50.68	14.58	10.46	7.75	11.63	2.47	0.05	1.73	0.15	0.17
35-2, 113–118	50.74	14.47	10.49	7.83	11.34	2.58	0.06	1.79	0.15	0.17
35-3, 21–27	50.02	14.49	10.80	8.26	11.27	2.64	0.06	1.76	0.15	0.17
35-4, 85–92	50.24	14.40	10.77	7.80	11.73	2.55	0.06	1.75	0.15	0.18
35-6, 47–53	50.72	14.45	10.97	7.35	11.35	2.54	0.06	1.83	0.16	0.20
36-3, 65–69	49.63	19.48	9.79	6.37	7.50	3.66	0.06	2.46	0.21	0.19
38-3, 18–23	49.89	15.15	10.71	7.85	11.19	2.58	0.08	1.78	0.16	0.18
38-6, 58–63	50.53	14.97	10.61	7.40	11.29	2.59	0.05	1.91	0.16	0.20
39-1, 26–32	50.33	14.84	10.74	7.69	11.16	2.54	0.05	1.89	0.16	0.20
39-1, 59–64	50.29	14.82	10.75	7.67	11.27	2.58	0.07	1.88	0.16	0.18

[a] Values in wt.%; normalized and corrected for carbonate contamination.

Table 3. Average compositions of basalt chemical types at DSDP Sites 482, 483, and 485.[a]

SiO_2	Al_2O_3	FeO*	MgO	CaO	Na_2O	K_2O	TiO_2	P_2O_5	MnO	Chemical Type
				(wt.%)						
Site 482										
50.58	14.71	10.25	7.96	11.63	2.58	0.09	1.82	0.16	0.21	A
50.47	15.14	10.12	8.04	11.95	2.48	0.06	1.44	0.12	0.18	F
50.85	14.94	9.94	8.20	11.93	2.46	0.04	1.35	0.11	0.18	B
51.20	14.70	10.03	8.16	12.00	2.30	0.06	1.28	0.11	0.17	C
50.35	15.54	9.88	7.42	12.25	2.65	0.04	1.56	0.14	0.18	D
50.67	14.67	10.32	7.85	11.54	2.67	0.06	1.89	0.17	0.18	E
50.79	14.40	11.40	6.87	11.02	2.86	0.11	2.15	0.20	0.19	G
50.55	14.96	10.05	8.31	11.90	2.46	0.05	1.43	0.11	0.18	H
Site 483										
51.04	15.25	9.17	8.04	12.31	2.64	0.06	1.24	0.09	0.16	B
50.78	14.77	9.97	7.86	12.17	2.73	0.06	1.39	0.10	0.17	C
49.84	16.87	8.27	9.09	12.38	2.27	0.04	1.01	0.07	0.16	D
51.09	16.47	8.48	7.44	10.99	3.19	0.16	1.85	0.18	0.15	E
50.06	15.70	10.36	7.22	12.07	2.62	0.06	1.58	0.13	0.20	I
50.34	15.08	10.72	7.14	11.80	2.61	0.09	1.86	0.17	0.20	F
50.33	14.54	11.41	7.28	10.97	2.80	0.10	2.18	0.21	0.19	H
50.40	15.04	10.25	7.56	11.93	2.65	0.08	1.73	0.15	0.21	J
50.36	14.67	10.71	7.67	11.63	2.72	0.09	1.82	0.16	0.19	K
50.42	14.91	10.52	7.60	11.60	2.65	0.11	1.81	0.16	0.23	L
50.42	15.59	9.63	7.64	11.94	2.68	0.12	1.62	0.15	0.20	M
50.87	14.71	9.99	7.75	12.37	2.65	0.05	1.33	0.10	0.17	Z
Site 485										
50.00	17.36	9.37	7.13	11.25	3.08	0.03	1.54	0.10	0.13	A
50.50	13.93	11.93	6.83	11.62	2.60	0.09	2.09	0.19	0.23	B
50.62	13.83	12.11	6.89	11.38	2.56	0.07	2.12	0.19	0.23	C
50.83	14.18	11.72	7.12	11.11	2.54	0.06	2.04	0.19	0.21	E
49.97	15.47	12.09	7.85	8.87	2.98	0.05	2.33	0.20	0.19	Z
50.26	14.83	11.40	7.07	10.76	2.93	0.14	2.24	0.20	0.17	H
50.10	14.71	11.07	7.82	11.12	2.62	0.13	2.05	0.18	0.19	I
50.68	14.59	10.68	7.78	11.48	2.60	0.06	1.79	0.15	0.18	J
49.95	19.61	9.85	6.41	7.55	3.68	0.06	2.48	0.21	0.19	K
50.44	15.00	10.74	7.68	11.27	2.58	0.06	1.87	0.16	0.19	L

[a] Values in wt.%, normalized and corrected for carbonate.

and the data used to refine the conclusions based on the major element variations. In general, the chemical types discussed above are also consistent with the trace element data. Incompatible (or "low-K_D") element enrichment factors are moreover consistent with the fractionation models based on major element mass balance considerations (Table 6). Rb and Nb values are generally below or close to detection limits and are therefore unreliable as petrogenetic indicators. The remaining elements reflect a wide range of solid–liquid partitioning behavior, from highly "compatible" to incompatible types. Zr, and to a lesser extent Y, are effectively excluded from olivine, plagioclase, and clinopyroxene during their crystallization in a tholeiite liquid. Sr is partitioned into plagioclase but not olivine or clinopyroxene and is thus a sensitive monitor for plagioclase fractionation. Cu and Zn do not discriminate significantly between the silicate phases and in general show compatible behavior. They are, however, very sensitive to sulfide fractionation. Ni and Cr are excluded from plagioclase but partition strongly, although differentially, into olivine and clinopyroxene. Taken together, the trace elements may be used to constrain models developed earlier from major element variation patterns.

As a general observation it is noted that the Zr/Ti ratios are not constant for all chemical types at any one site and appear to distinguish broader groupings of these types. The Zr/Y ratios also vary between types for equivalent values of Zr and reflect a significant positive correlation with Zr content. Zr/Y ratios of about 2.4, corresponding to 50–60 ppm Zr, increase to about 3.1 for 140–150 ppm Zr. These observations are important in evaluating the relative significance of fractional crys-

Table 4. Trace element abundances in fresh basalts from DSDP Sites 482, 483, and 485.

Sample (interval in cm)	Cu	Zn	Rb	Nb	Cr	Ni	Sr	Y	Zr
					(ppm)				
Hole 482B									
13-1, 99–104	56	85	4	7	272	70	107	39	113
14-1, 91–94	84	84	2	8	254	102	91	35	86
14-1, 132–137	72	76	1	9	240	90	97	32	83
14-3, 2–6	76	82	2	8	230	90	92	33	84
14-4, 16–20	70	90	2	8	240	83	93	33	84
15-1, 12–16	68	78	3	9	236	91	92	34	86
16-4, 100–104	65	74	4	6	180	57	87	31	75
20-1, 27–30	92	93	3	10	202	76	116	35	100
20-3, 144–147	72	87	1	8	201	68	112	34	96
21-2, 19–23	80	78	5	8	193	56	104	30	80
21-3, 58–63	79	86	1	8	231	58	124	36	107
22-2, 67–72	82	89	2	8	242	62	123	35	106
22-2, 130–136	71	83	0	6	226	57	124	35	106
22-3, 103–107	66	80	1	8	222	71	120	35	102
22-4, 97–102	82	85	1	8	244	67	122	35	105
24-3, 110–115	68	87	7	8	191	63	110	41	123
Hole 482C									
10-1, 0–4	71	89	6	9	260	61	111	39	123
10-1, 9–12	79	90	3	9	275	67	106	41	119
10-1, 12–16	78	105	0	8	278	64	107	41	118
10-3, 11–14	75	78	7	8	285	73	104	37	111
11-3, 65–69	94	97	1	9	295	71	104	38	113
12-1, 92–118	72	70	1	9	185	57	89	32	77
13-1, 10–15	89	83	3	7	176	58	93	31	77
14-1, 13–18	70	79	3	7	166	54	90	32	76
15-1, 114–118	80	85	1	7	188	55	97	32	79
Hole 482D									
8-1, 24–29	70	82	4	8	264	71	106	40	116
8-1, 65–72	77	94	6	8	296	69	111	39	116
10-1, 106–109	70	84	3	9	228	91	92	33	84
10-1, 111–114	78	90	2	7	299	73	111	39	116
10-2, 70–72	71	89	1	8	249	66	106	40	115
10-2, 128–130	88	92	4	9	263	66	108	40	121
10-3, 25–27	67	87	1	8	206	63	107	43	127
10-3, 93–97	87	83	4	10	235	93	92	33	85
12-1, 28–32	92	91	3	8	238	90	91	33	84
12-3, 27–31	78	80	2	7	192	55	90	32	77
13-1, 49–51	78	83	1	8	185	56	98	32	80
13-1, 98–101	102	90	3	9	191	57	92	32	78
13-1, 128–134	81	78	2	7	179	61	92	32	79
Hole 482F									
5-1, 133–139	95	97	2	9	163	64	104	40	117
11-1, 125–128	93	87	5	8	288	93	89	33	84
Hole 483									
14-1, 58–68	99	73	3	8	363	62	117	28	74
15-1, 93–97	91	65	2	8	348	65	114	28	73
16-2, 64–70	81	84	1	8	230	52	94	32	77
16-2, 99–100	91	82	4	8	235	54	98	30	77
16-3, 2–6	67	73	0	8	279	56	96	30	73
17-2, 13–17	96	62	1	8	315	108	99	25	59
17-2, 17–21	88	67	2	7	360	148	81	23	53
18-4, 131–134	104	95	4	9	285	96	174	37	117
21-1, 49–55	66	89	2	9	170	68	101	43	127
21-1, 57–61	81	92	4	9	183	63	103	43	125
21-3, 6–9	85	97	6	10	183	63	104	42	128
22-2, 68–72	85	92	2	9	261	63	101	38	110
22-2, 74–77	68	81	2	8	258	79	98	39	111
22-2, 85–88	68	87	2	9	257	77	98	38	110
22-2, 88–93	90	92	3	9	257	78	103	39	112
22-2, 94–99	62	84	2	8	243	80	101	39	112
23-1, 10–16	81	96	2	9	257	77	103	39	113
24-1, 52–57	82	111	3	10	167	66	115	48	153
24-2, 35–40	79	100	3	9	170	67	105	46	141
25-2, 61–66	94	101	8	10	163	75	104	45	141

Table 4. (Continued).

Sample (interval in cm)	Cu	Zn	Rb	Nb	Cr	Ni	Sr	Y	Zr
					(ppm)				
Hole 483 (Cont.)									
26-1, 59-63	75	103	2	10	166	65	107	46	140
26-2, 40-44	76	100	2	9	164	64	106	46	137
26-3, 124-130	65	96	1	10	153	68	107	48	144
Hole 483B									
4-1, 26-30	88	70	4	8	351	64	111	28	74
7-1, 7-12	77	84	1	7	226	50	93	32	78
7-1, 26-31	127	92	3	9	233	52	91	31	74
7-2, 56-61	80	79	4	9	220	55	93	31	75
7-3, 2-6	80	80	1	6	210	53	95	32	75
8-1, 29-35	100	71	0	8	320	109	118	25	60
8-1, 55-61	82	71	0	8	294	102	90	23	58
8-1, 120-126	87	73	2	8	325	104	93	25	59
8-2, 121-126	108	76	2	7	301	87	165	26	63
8-7, 2-20	94	66	5	8	290	114	132	26	65
12-1, 92-95	71	87	3	7	189	74	115	36	98
13-1, 38-44	70	93	6	10	182	67	102	42	125
13-1, 60-64	72	95	2	10	182	63	103	43	126
13-1, 60-64	83	98	3	9	187	66	105	43	129
13-1, 66-67	85	89	8	9	182	84	95	48	142
13-1, 66-67	59	93	2	10	185	58	100	43	127
13-1, 74-79	65	87	5	9	180	54	101	43	126
13-1, 92-98	71	91	2	9	214	73	98	40	116
13-1, 108-119	65	94	2	10	182	62	99	42	122
13-1, 115-122	65	94	3	8	169	59	102	43	128
13-1, 115-122	61	93	1	9	189	64	103	42	124
13-1, 124-131	55	96	1	10	194	66	103	42	124
13-1, 124-131	99	96	7	8	190	65	101	42	125
13-1, 134-139	79	95	6	9	186	65	103	43	130
14-1, 130-133	88	91	1	9	207	81	102	40	118
18-1, 49-52	76	108	3	8	152	56	105	47	148
18-1, 103-107	70	94	5	10	152	66	104	45	139
18-2, 18-22	81	103	3	10	166	66	106	47	142
19-2, 17-21	73	105	3	9	159	59	107	47	142
19-2, 104-108	67	103	6	10	158	68	110	48	149
19-3, 8-12	69	94	5	10	163	77	113	46	143
20-1, 14-19	64	102	1	9	164	89	107	44	139
20-1, 94-99	78	102	4	10	175	86	110	45	140
20-2, 9-14	79	98	3	10	180	75	106	45	138
20-2, 16-21	80	99	2	8	186	70	103	46	136
20-2, 25-30	85	107	3	10	170	69	106	45	138
20-2, 37-42	83	102	5	10	162	68	103	46	139
20-2, 50-59	67	100	5	10	171	72	109	46	145
20-2, 50-59	68	103	2	10	168	71	105	46	141
20-2, 50-59	88	114	3	10	170	66	109	48	144
20-2, 142-146	59	100	1	9	227	73	101	44	130
21-2, 57-61	82	93	3	10	206	70	112	39	110
22-1, 26-32	86	98	2	9	189	64	111	39	109
22-2, 63-67	86	85	3	7	214	77	112	36	100
22-2, 77-82	69	90	1	9	196	70	108	37	103
23-4, 19-24	84	88	2	9	211	74	109	35	102
25-2, 22-28	75	101	1	9	155	60	119	43	122
25-2, 39-45	80	96	4	9	177	63	113	40	116
26-2, 42-47	66	90	7	8	165	61	108	40	105
26-2, 126-137	73	86	6	10	174	60	109	39	105
27-1, 12-18	82	92	4	9	184	66	119	38	116
27-1, 114-119	67	93	1	9	168	62	110	38	112
27-2, 95-101	68	93	4	10	163	60	108	39	115
27-3, 94-98	63	92	1	10	142	54	105	39	110
27-4, 74-80	76	91	5	9	213	67	107	38	110
28-1, 42-59	56	83	3	9	217	74	106	38	110
28-1, 123-128	76	82	3	8	246	84	105	36	105
28-2, 28-32	65	82	2	10	264	91	104	36	101
28-3, 37-40	74	82	4	8	251	95	104	36	102
29-1, 10-15	78	85	2	9	232	88	105	37	105
29-1, 26-31	69	81	2	9	204	77	108	38	109

Table 4. (Continued).

Sample (interval in cm)	Cu	Zn	Rb	Nb	Cr	Ni	Sr	Y	Zr
					(ppm)				
Hole 483B (Cont.)									
29-1, 40-45	62	90	2	8	201	68	108	38	108
29-1, 55-57	84	94	0	10	187	68	110	38	112
29-1, 57-62	99	98	6	10	210	79	123	40	121
29-1, 57-62	56	88	1	9	192	66	111	40	111
30-3, 13-16	70	89	1	9	230	82	111	39	110
30-3, 18-22	67	84	3	10	232	80	110	39	111
31-3, 20-25	72	85	2	8	298	106	120	38	104
32-1, 1-6	67	80	6	9	296	117	115	34	99
32-1, 27-31	64	77	3	9	293	97	119	35	100
32-1, 44-50	80	88	3	8	300	104	116	35	100
32-1, 90-94	84	100	2	10	298	103	117	36	101
32-1, 90-94	74	84	2	10	303	111	118	36	102
32-1, 84-88	72	82	3	8	311	133	118	34	99
Hole 483C									
4-4, 58-66	70	81	5	8	166	60	87	35	96
Hole 485A									
11-3, 57-60	122	94	2	8	423	244	181	35	98
11-3, 68-73	84	69	4	7	392	208	108	31	91
11-3, 116-121	79	71	2	6	417	233	184	32	92
12-1, 10-16	55	98	1	8	160	62	95	46	124
12-1, 76-82	56	101	0	9	155	58	90	46	126
12-1, 114-120	70	99	3	8	157	60	92	45	124
13-1, 11-18	70	99	2	9	172	71	96	45	119
13-1, 110-117	50	95	1	6	157	69	101	45	120
17-1, 77-82	44	87	3	10	221	86	146	42	136
23-1, 50-56	52	54	8	8	198	68	110	47	141
23-1, 50-56	97	78	13	9	199	75	123	45	139
23-1, 50-56	64	78	4	9	215	76	112	48	144
23-1, 148-149	47	94	2	8	212	70	107	46	136
23-2, 16-22	79	94	4	10	220	72	111	47	137
23-3, 120-125	59	96	2	9	250	71	110	44	137
25-1, 117-143	58	94	2	10	217	77	102	46	135
29-1, 2-8	80	111	5	8	216	99	117	46	141
29-1, 89-93	60	81	4	10	226	90	108	45	142
29-2, 143-148	91	98	5	10	191	67	103	43	130
29-3, 10-16	63	80	7	8	266	77	95	44	139
30-2, 96-101	107	110	5	10	329	57	91	48	146
30-3, 38-41	78	78	4	9	651	86	90	39	112
30-3, 44-49	31	66	2	7	526	79	97	40	108
30-4, 8-13	28	77	3	9	160	78	107	41	127
31-1, 62-67	58	86	1	9	405	96	89	34	90
31-3, 34-39	63	109	4	7	222	101	100	41	117
32-1, 55-61	45	55	5	10	180	66	110	48	141
32-2, 99-105	64	105	5	9	180	129	99	42	123
32-3, 47-51	73	104	4	7	252	124	98	41	120
32-5, 9-14	44	90	4	9	240	123	98	43	128
32-6, 52-57	73	103	5	10	198	110	97	46	137
33-1, 2-9	68	121	6	8	216	111	94	46	137
33-1, 74-79	52	123	5	10	223	120	96	45	134
33-2, 26-33	72	125	10	8	234	121	97	45	127
33-2, 72-78	74	97	9	8	220	104	92	44	137
33-2, 88-94	65	96	5	10	228	100	101	47	140
34-1, 86-90	74	90	1	9	269	71	102	38	113
34-2, 96-102	65	85	1	7	256	69	95	39	110
35-1, 135-142	72	86	3	8	250	71	95	38	106
35-2, 113-118	70	83	3	8	248	71	95	39	109
35-3, 21-27	60	74	2	7	240	69	133	38	109
35-4, 85-92	70	88	2	10	260	70	92	39	109
35-6, 47-53	70	87	2	8	254	67	95	40	111
36-3, 65-69	91	161	2	7	251	107	144	44	140
38-3, 18-23	52	89	3	8	212	84	102	39	109
38-6, 58-63	61	87	4	9	200	81	101	41	118
39-1, 26-32	40	81	2	9	222	76	104	40	114
39-1, 59-64	70	94	7	8	202	77	95	39	114

Table 5. Trace element ratios in fresh basalts from DSDP Sites 482, 483, and 485.

Sample (interval in cm)	1/Ni	1/Sr	1/Y	Zr/Y	Zr/Nb	Ti/Y	Zr/SR	Zr/Ni	Y/Nb
Hole 482B									
13-1, 99-104	14.29	9.35	25.64	2.90	16.14	267.3	1.06	1.61	5.57
14-1, 91-94	9.80	10.99	28.57	2.46	10.75	240.6	0.95	0.84	4.38
14-1, 132-137	11.11	10.31	31.25	2.59	9.22	252.1	0.86	0.92	3.56
14-3, 2-6	11.11	10.87	30.30	2.55	10.50	249.8	0.91	0.93	4.13
14-4, 16-20	12.00	10.75	30.30	2.55	10.50	251.6	0.90	1.01	4.13
15-1, 12-16	10.99	10.87	29.41	2.53	9.56	251.1	0.93	0.95	3.78
16-4, 100-104	17.54	11.49	32.26	2.42	12.50	239.4	0.86	1.32	5.17
20-1, 27-30	13.15	8.62	28.57	2.86	10.00	264.1	0.86	1.32	3.50
20-3, 144-147	13.04	8.90	27.78	2.67	12.00	245.4	1.10	1.68	4.50
21-2, 19-23	17.86	9.62	33.33	2.30	10.00	248.0	0.77	1.43	3.75
21-3, 58-63	17.24	8.06	27.78	2.97	13.38	258.5	0.86	1.84	4.50
22-2, 67-72	16.13	8.13	28.57	3.03	13.25	260.8	0.86	1.71	4.38
22-2, 130-136	17.54	8.06	28.57	3.03	17.67	264.2	0.85	1.86	5.83
22-3, 103-107	14.08	8.25	28.57	2.91	12.75	250.7	0.85	1.44	4.38
22-4, 97-102	14.92	8.20	28.57	3.00	13.13	260.8	0.86	1.57	4.38
24-3, 110-115	15.87	9.09	24.39	3.00	15.38	265.7	1.12	1.95	5.13
Hole 482C									
10-1, 0-4	16.39	9.01	25.64	3.15	13.67	280.9	1.11	2.02	4.33
10-1, 9-12	14.93	9.43	24.39	2.90	13.22	260.0	1.12	1.78	4.56
10-1, 12-16	15.63	9.35	24.39	2.88	14.75	261.4	1.10	1.84	5.13
10-3, 11-14	13.70	9.62	27.03	3.00	13.88	270.6	1.07	1.52	4.63
11-3, 65-69	14.08	9.62	26.32	2.97	12.56	272.8	1.09	1.59	4.22
12-1, 92-118	17.54	11.23	31.25	2.41	8.56	233.7	0.87	1.35	3.56
13-1, 10-15	17.24	10.75	32.26	2.48	11.00	248.9	0.83	1.33	4.43
14-1, 13-18	18.52	11.11	31.25	2.38	10.86	241.1	0.84	1.41	4.57
15-1, 114-118	18.18	10.31	31.25	2.47	11.29	244.8	0.81	1.44	4.57
Hole 482D									
8-1, 24-29	14.08	9.43	25.00	2.90	14.50	257.7	1.00	1.63	5.00
8-1, 65-72	14.49	9.01	25.65	2.97	14.50	264.3	1.05	1.68	4.88
10-1, 106-109	10.99	10.87	30.30	2.55	9.33	249.8	0.91	0.92	3.67
10-1, 111-114	13.70	9.01	25.64	2.97	16.57	270.3	1.05	1.59	5.57
10-2, 70-72	15.15	9.43	25.00	2.88	14.38	265.0	1.08	1.74	5.00
10-2, 128-130	15.15	9.26	25.00	3.02	13.44	273.9	1.12	1.83	4.44
10-3, 25-27	15.87	9.35	23.26	2.95	15.88	271.2	1.19	2.02	5.38
10-3, 93-97	10.75	10.87	30.30	2.58	8.50	255.2	0.92	0.91	3.30
12-1, 28-32	11.11	10.99	30.30	2.55	10.50	249.8	0.92	0.93	4.13
12-3, 27-31	18.18	11.11	31.25	2.41	11.00	239.3	0.86	1.40	4.57
13-1, 49-51	17.86	10.20	31.25	2.50	10.00	246.6	0.82	1.43	4.00
13-1, 98-101	17.54	10.87	31.25	2.44	8.67	235.6	0.85	1.37	3.56
13-1, 128-134	16.39	10.87	31.25	2.47	11.29	242.9	0.86	1.30	4.57
Hole 482F									
5-1, 133-139	15.63	9.62	25.00	2.92	13.00	267.7	1.13	1.83	4.14
11-1, 125-128	10.75	11.24	30.30	2.55	10.50	251.6	0.94	0.90	4.13
Hole 483									
14-1, 58-68	16.13	8.55	35.71	2.64	9.25	254.5	0.63	1.19	3.50
15-1, 93-97	15.38	8.77	35.71	2.61	9.13	256.6	0.64	1.12	3.50
16-2, 64-70	19.23	10.64	31.25	2.41	9.63	259.0	0.82	1.48	4.00
16-2, 99-100	18.52	10.20	33.33	2.57	9.63	274.8	0.79	1.43	3.75
16-3, 2-6	17.86	10.42	33.33	2.43	9.13	259.1	0.76	1.30	3.75
17-2, 13-17	9.26	10.10	40.00	2.36	7.38	230.8	0.60	0.55	3.13
17-2, 17-21	6.76	11.90	43.48	2.30	7.57	225.3	0.46	0.52	3.29
18-4, 131-134	10.42	5.75	27.03	3.16	14.78	286.5	0.76	1.39	4.11
21-1, 49-55	14.71	9.90	23.26	2.95	14.11	258.8	1.26	1.87	4.78
21-1, 57-61	15.87	9.71	23.26	2.91	13.89	257.5	1.21	1.98	4.78
21-3, 6-9	15.87	9.62	23.81	3.05	12.80	272.0	1.23	2.03	4.20
22-2, 68-72	15.87	9.90	26.32	2.89	12.22	257.3	1.09	1.75	4.22
22-2, 74-77	12.66	10.20	25.64	2.85	13.88	250.7	1.13	1.41	4.88
22-2, 85-88	12.99	10.20	26.32	2.89	12.22	254.2	1.12	1.43	4.22
22-2, 88-93	12.82	9.71	25.64	2.87	12.44	255.2	1.09	1.44	4.33
22-2, 94-99	12.50	9.90	25.64	2.87	14.00	253.7	1.11	1.40	4.88
23-1, 10-16	12.99	9.71	25.64	2.90	12.56	259.7	1.10	1.47	4.33
24-1, 52-57	15.15	8.70	20.83	3.19	15.30	284.6	1.33	2.32	4.80
24-2, 35-40	14.93	9.52	21.74	3.07	15.67	272.7	1.34	2.10	5.11
25-2, 61-66	13.33	9.62	22.22	3.13	14.10	276.1	1.36	1.88	4.50
26-1, 59-63	15.38	9.35	21.74	3.04	14.00	272.7	1.31	2.15	4.60
26-2, 40-44	15.63	9.43	21.74	2.98	15.22	266.3	1.29	2.14	5.11
26-3, 124-130	17.24	9.35	20.83	3.00	14.40	266.2	1.35	2.48	4.80
Hole 483B									
4-1, 26-30	15.63	9.01	35.71	2.64	9.25	256.6	0.67	1.16	3.50
7-1, 7-12	20.00	10.75	31.25	2.44	11.14	259.5	0.84	1.56	4.57
7-1, 26-31	19.23	10.99	32.26	2.39	8.22	256.5	0.81	1.42	3.44
7-2, 56-61	18.18	10.75	32.26	2.42	8.33	256.5	0.81	1.36	3.44
7-3, 2-6	18.87	10.53	31.25	2.34	12.50	252.1	0.79	1.42	5.33
8-1, 29-35	9.17	8.47	40.00	2.40	7.50	233.2	0.51	0.55	3.13
8-1, 55-61	9.80	11.11	43.48	2.32	9.67	245.8	0.64	0.57	3.83
8-1, 120-126	9.62	10.75	40.00	2.36	7.38	233.2	0.63	0.57	3.13
8-2, 121-126	9.49	6.06	38.46	2.42	9.00	242.3	0.38	0.72	3.71
8-7, 2-20	8.77	7.58	38.46	2.50	8.13	237.8	0.49	0.57	3.25
12-1, 92-95	13.51	8.70	27.78	2.72	14.00	255.2	0.85	1.32	5.14
13-1, 38-44	14.93	9.80	23.81	2.98	12.50	262.2	1.22	1.87	4.20
13-1, 60-64	15.88	9.71	23.26	2.93	12.60	258.8	1.22	2.00	4.30
13-1, 60-64	15.15	9.52	23.26	3.00	14.33	263.0	1.23	1.95	4.78
13-1, 66-67	11.90	10.53	20.83	2.96	15.78	260.0	1.49	1.69	4.30
13-1, 66-67	17.24	10.00	23.26	2.95	12.70	263.0	1.27	2.19	5.33
13-1, 74-79	18.52	9.90	23.26	2.93	14.00	258.8	1.25	2.33	4.78
13-1, 92-98	13.70	10.20	25.00	2.90	12.89	256.2	1.18	1.59	4.44
13-1, 108-119	16.13	10.10	23.81	2.90	12.20	256.6	1.23	1.97	4.20
13-1, 115-122	16.95	9.80	23.26	2.98	16.00	267.1	1.25	2.17	4.67
13-1, 115-122	15.63	9.71	23.81	2.95	13.78	263.6	1.20	1.94	4.67
13-1, 124-131	15.15	9.71	23.81	2.95	12.40	263.6	1.20	1.88	4.20
13-1, 124-131	15.38	9.90	23.81	2.98	15.63	255.0	1.24	1.92	5.25
13-1, 134-139	15.38	9.71	23.26	3.02	14.44	268.4	1.26	2.00	5.38
14-1, 134-139	12.35	9.80	25.00	2.95	13.11	259.1	1.16	1.46	5.04
18-1, 49-52	18.18	9.52	21.28	3.15	18.50	278.2	1.41	2.64	5.88
18-1, 103-107	15.15	9.62	22.22	3.09	13.90	276.1	1.34	2.11	4.50

Table 5. (Continued).

Sample (interval in cm)	1/Ni	1/Sr	1/Y	Zr/Y	Zr/Nb	Ti/Y	Zr/SR	Zr/Ni	Y/Nb
Hole 483B (Cont.)									
18-2, 18-22	15.15	9.43	21.28	3.02	14.20	270.6	1.34	2.15	4.70
19-2, 17-21	16.95	9.35	21.28	3.02	15.78	268.1	1.33	2.41	5.22
19-2, 104-108	14.71	9.09	20.83	3.10	14.90	273.6	1.35	2.19	4.80
19-3, 8-12	12.99	8.85	21.74	3.11	14.30	274.0	1.27	1.86	4.60
20-1, 14-19	11.24	9.35	22.73	3.16	15.44	281.1	1.30	1.56	4.89
20-1, 94-99	11.63	9.09	22.22	3.11	14.00	273.5	1.27	1.63	4.50
20-2, 9-14	13.33	9.43	22.22	3.07	13.80	270.9	1.30	1.84	4.50
20-2, 16-21	14.29	9.71	21.74	2.96	17.00	262.4	1.28	1.94	5.75
20-2, 25-30	14.49	9.43	22.22	3.07	13.80	277.4	1.31	2.00	4.50
20-2, 37-42	14.71	9.71	21.74	3.02	13.90	270.1	1.35	2.04	4.60
20-2, 50-59	13.89	9.17	21.74	3.15	14.50	280.4	1.33	2.01	4.60
20-2, 50-59	14.08	9.52	21.74	3.07	14.10	274.0	1.34	1.99	4.60
20-2, 50-59	15.15	9.17	20.83	3.00	14.40	263.8	1.32	2.18	4.80
20-2, 142-146	13.70	9.90	22.73	2.95	14.44	270.4	1.29	1.78	4.89
21-2, 57-61	14.29	8.93	25.64	2.82	11.00	268.8	0.98	1.57	3.90
22-1, 26-32	15.63	9.01	25.64	2.79	12.11	270.3	0.98	1.70	4.33
22-2, 63-67	12.99	8.93	27.78	2.78	14.29	263.4	0.89	1.30	5.14
22-2, 77-82	14.29	9.71	27.03	2.78	11.44	264.2	1.00	1.47	4.11
23-4, 19-24	13.51	9.17	28.57	2.91	11.22	281.0	0.94	1.38	3.89
25-2, 22-28	16.67	8.40	23.26	2.84	13.56	269.8	1.03	2.03	4.78
25-2, 39-45	15.87	8.85	25.00	2.90	12.89	270.9	1.03	1.84	4.44
26-2, 42-47	16.39	9.26	25.00	2.63	13.13	254.7	0.97	1.72	5.00
26-2, 126-137	16.67	9.17	25.64	2.69	10.50	256.7	0.96	1.75	3.90
27-1, 12-18	15.15	8.40	26.32	3.05	12.89	288.3	0.97	1.75	4.22
27-1, 114-119	16.13	9.09	26.32	2.95	12.44	283.6	1.02	1.81	4.22
27-2, 95-101	16.67	9.26	15.64	2.95	11.50	280.9	1.06	1.92	3.90
27-3, 94-98	18.52	9.52	25.64	2.82	11.00	275.0	1.05	2.04	3.90
27-4, 74-80	14.93	9.35	26.32	2.89	12.22	271.2	1.03	1.64	4.22
28-1, 42-59	13.51	9.43	26.32	2.89	12.22	272.8	1.04	1.49	4.22
28-1, 123-128	11.90	9.52	27.78	2.92	13.13	274.8	1.00	1.24	4.50
28-2, 28-32	10.99	9.62	27.78	2.81	10.10	268.3	1.00	1.11	3.60
28-3, 37-40	10.53	9.62	27.78	2.83	12.75	268.3	0.97	1.07	4.50
29-1, 10-15	11.36	9.52	27.03	2.84	11.67	267.4	0.98	1.19	4.11
29-1, 26-31	12.99	9.26	26.32	2.87	12.11	269.7	1.00	1.42	4.22
29-1, 40-45	14.71	9.26	26.32	2.84	13.50	271.2	1.01	1.59	4.75
29-1, 55-57	14.71	9.09	26.32	2.95	11.20	277.4	1.00	1.65	3.80
29-1, 57-62	12.66	8.13	25.00	3.02	12.10	287.1	1.02	1.53	4.00
29-1, 57-62	15.15	9.01	25.00	2.77	12.33	263.5	0.98	1.62	4.44
30-3, 13-16	12.20	9.01	25.64	2.82	12.22	265.8	0.99	1.34	4.33
30-3, 18-22	12.50	9.09	25.64	2.85	11.10	267.3	1.01	1.39	3.90
31-3, 20-25	9.43	8.33	26.32	2.74	13.00	258.8	0.87	0.98	4.75
32-1, 1-6	8.55	8.70	29.41	2.91	11.00	273.7	0.87	0.85	3.78
32-1, 27-31	10.31	8.40	28.57	2.86	11.11	262.5	0.84	1.03	3.89
32-1, 44-50	9.62	8.62	28.57	2.81	12.20	262.5	0.85	1.02	4.38
32-1, 90-94	9.71	8.55	27.78	2.81	10.10	261.7	0.86	0.98	3.60
32-1, 90-94	9.01	8.47	27.78	2.83	10.20	260.1	0.86	0.92	3.60
32-1, 84-88	7.52	8.47	29.41	2.91	12.38	271.9	0.84	0.74	4.25
Hole 483C									
4-4, 58-66	16.67	11.49	28.57	2.74	12.00	222.2	1.10	1.60	4.38
Hole 485A									
11-3, 57-60	4.10	5.52	28.57	2.80	12.25	260.8	0.54	0.40	4.38
11-3, 68-73	4.81	9.25	32.26	2.94	13.00	269.7	0.84	0.44	4.43
11-3, 116-121	4.29	5.43	31.25	2.88	15.33	268.7	0.50	0.39	5.33
12-1, 10-16	16.13	10.53	21.74	2.70	15.50	261.2	1.31	2.00	5.75
12-1, 76-82	17.24	11.11	21.74	2.74	14.00	262.4	1.40	2.17	5.11
12-1, 114-120	16.66	10.87	22.22	2.76	15.50	265.7	1.35	2.07	5.63
13-1, 11-18	14.08	10.42	22.22	2.64	13.22	252.6	1.24	1.68	5.00
13-1, 110-117	14.49	9.90	22.22	2.67	14.60	257.8	1.19	1.74	5.50
17-1, 77-82	11.63	6.85	23.81	3.24	13.60	300.0	0.93	1.58	4.20
23-1, 50-56	14.71	9.09	21.28	3.00	17.63	271.9	1.28	2.07	5.88
23-1, 50-56	13.33	8.13	22.22	3.09	15.44	280.0	1.13	1.85	5.00
23-1, 50-56	13.16	8.93	20.83	3.00	16.00	273.6	1.29	1.89	5.33
23-1, 148-149	14.29	9.35	21.74	2.96	17.00	271.4	1.27	1.94	5.75
23-2, 16-22	13.89	9.01	21.28	2.91	13.70	272.7	1.23	1.90	4.70
23-3, 120-125	14.08	9.09	22.73	3.11	15.22	294.5	1.25	1.93	4.89
25-1, 117-143	12.99	9.80	21.74	2.93	13.50	270.1	1.32	1.75	4.60
29-1, 2-8	10.10	8.55	21.74	3.07	17.63	281.7	1.21	1.42	5.75
29-1, 89-93	11.11	9.26	22.22	3.16	14.20	291.8	1.31	1.58	4.50
29-2, 143-148	14.93	9.71	23.26	3.02	13.00	265.7	1.26	1.94	4.30
29-3, 10-16	12.99	10.53	22.73	3.16	17.38	295.8	1.46	1.81	5.50
30-2, 96-101	17.54	10.99	20.83	3.04	14.60	238.0	1.60	2.56	4.80
30-3, 38-41	11.63	11.11	25.64	2.87	12.44	265.8	1.24	1.30	4.33
30-3, 44-49	12.66	10.31	25.00	2.70	15.43	262.1	1.11	1.26	5.71
30-4, 8-13	12.82	9.35	24.39	3.10	14.11	274.3	1.19	1.68	4.56
31-1, 62-67	10.42	11.24	29.41	2.65	10.00	251.1	1.01	0.94	3.78
31-3, 34-39	9.90	10.00	24.39	2.85	16.71	268.6	1.17	1.16	5.86
32-1, 55-61	15.15	9.09	20.83	2.94	14.10	257.6	1.28	2.14	4.80
32-2, 99-105	7.75	10.10	23.81	2.93	13.67	272.0	1.24	0.95	4.67
32-3, 47-51	8.06	10.20	24.39	2.93	17.14	278.7	1.22	0.97	5.86
32-5, 9-14	8.13	10.20	23.26	2.98	14.22	273.9	1.31	1.04	4.78
32-6, 52-57	9.09	10.31	21.74	2.98	13.70	277.8	1.41	1.25	4.60
33-1, 2-9	9.01	10.64	21.74	2.98	17.13	271.4	1.46	1.23	5.75
33-1, 74-79	8.33	10.42	22.22	2.98	13.40	277.4	1.40	1.12	4.50
33-2, 26-33	8.26	10.31	22.22	2.82	15.88	273.5	1.31	1.05	5.63
33-2, 72-78	9.62	10.87	22.73	3.11	17.13	285.1	1.49	1.32	5.50
33-2, 88-94	10.00	9.90	21.28	2.98	14.00	266.9	1.39	1.40	4.70
34-1, 86-90	14.08	9.80	26.32	2.97	12.56	282.1	1.11	1.59	4.22
34-2, 96-102	14.49	10.53	25.64	2.82	15.71	261.2	1.16	1.59	5.57
35-1, 135-142	14.08	10.53	26.32	2.79	13.25	265.0	1.12	1.49	4.75
35-2, 113-118	14.08	10.53	25.64	2.79	13.63	265.8	1.15	1.54	4.88
35-3, 21-27	14.49	7.52	26.32	2.87	15.57	266.6	0.89	1.58	5.43
35-4, 85-92	14.29	10.87	25.64	2.79	10.90	259.7	1.18	1.56	3.90
35-6, 47-53	14.93	10.53	25.00	2.77	13.88	265.0	1.17	1.66	5.00
36-3, 65-69	9.35	6.94	22.73	3.18	20.00	303.8	0.97	1.31	6.29
38-3, 18-23	11.90	9.80	25.64	2.79	13.63	264.3	1.07	1.30	4.88
38-6, 58-63	12.35	9.90	24.39	2.88	13.11	271.5	1.17	1.46	4.50
39-1, 26-32	13.16	9.62	25.00	2.85	12.67	272.4	1.10	1.50	4.44
39-1, 59-64	12.99	10.53	25.64	2.92	14.25	280.9	1.20	1.48	4.88

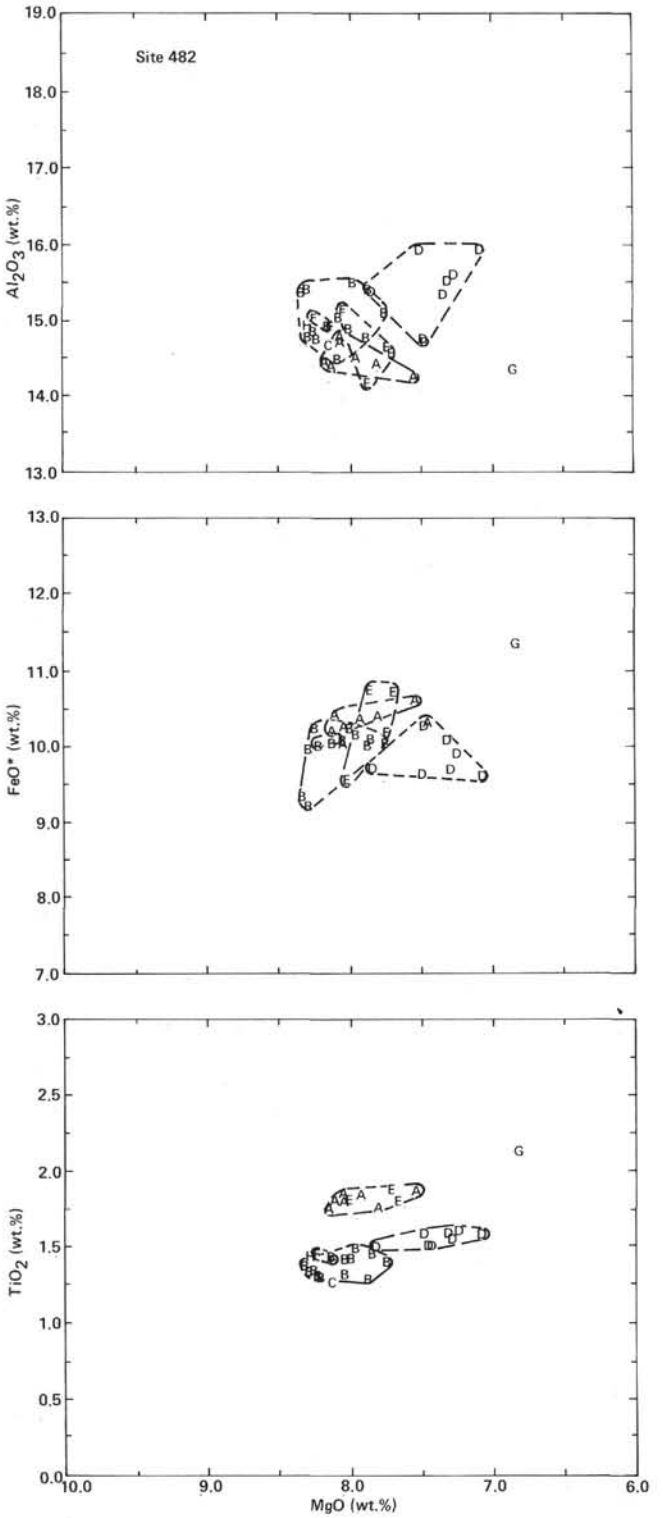

Figure 3. Al_2O_3, FeO*, and TiO_2 versus MgO for Site 482. (Dashed lines indicate chemical types. Types A, B, C, E, and F are sparsely phyric or aphyric; Type D is moderately plagioclase-phyric.)

tallization, variable partial melting, and magma mixing in determining the overall chemical variation at these sites.

Variation diagrams for Ti/Zr, Y/Zr, Sr/Zr, and Ni/Cr are given in Figures 6 to 9 for all three sites. The data are labelled according to chemical type.

1) Ti/Zr: Ti and Zr predictably show a positive covariance (Fig. 6), with the exception of Site 485 Type I which may reflect minor fractionation of magnetite. The Ti/Zr ratios appear uniform for Site 482 and 485 basalts but are distinctly variable for Site 483 and appear to depend on chemical type. The "upper" massive types (D, B, and C) show between-type variation, but the "lower" massive (H and K) and pillow (F, I, J, L, and M) types can be divided into at least two series: namely, H–F and K–L–M–J–I, respectively. Discrepancies between the series are not compatible with simple fractionation or single-stage mixing models and are tentatively attributed to differences in source composition and/or the degree of partial melting.

2) Y/Zr: Y variation for Site 482 (Fig. 7) distinguishes Types B, F, and D from Types A and E, which overlap. The Site 483 data show similar patterns in which the high Zr types (F, H, I, J, K, L, and M), which are interlayered "lower" massive and pillow sequences, are distinct from the low-Zr types (B, C, and D), the "upper" massive units. A similar pattern is also observed for Site 485 despite complex variation in Cooling Unit 9 (Type I). Cooling Unit 5 may reflect anomalous Y/Zr ratios. As noted above, the basalts at all sites reflect increasing Y/Zr ratios with increasing Zr content. This is best observed in the Site 483 data. However, no definitive between-site source differences are confirmed. Further low-K_d element data are needed to test for this possibility.

3) Sr/Zr: The variation of Sr at all of the sites (Fig. 8) corresponds closely to that observed for Al_2O_3 (Figs. 3–5) and is consistent with the inferred effects of plagioclase. Type D at Site 482 is plagioclase-phyric and shows Sr enrichment compared to aphyric Types A and E. Types B and F are unlikely to be related to Types A and E by simple fractionation unless olivine control was dominant or plagioclase was accumulated during the removal of the mafic phases. The variation at Site 483 shows similar patterns, but an apparent contradiction exists between the Sr enrichment in Chemical Types D, H, and K (and major element mass balance requirements; see Table 6) and their aphyric to very sparsely phyric petrography, which shows no evidence of significant plagioclase accumulation. Major element mass balance considerations and Sr variation imply concurrent accumulation of plagioclase with mafic phase fractionation. The pillow sequences making up Chemical Types F, J, L, and M also reflect similar mass balance relations, although the required enrichment in plagioclase is significantly less (Fig. 8; Table 6).

Sr variation in the Site 485 basalts is somewhat more erratic but loosely resembles that at the other sites. Cooling Units 1(A), 8(H), 10(J), and subunits of 9(I) reflect steep Sr/Zr trends similar to that shown by Type D at Site 483. However, some of these units (8–10) reflect modal plagioclase indicative of accumulation.

4. Ni/Cr: Ni/Cr ratios are insensitive to the fractionation and accumulation of plagioclase; their variation reflects the crystallization and redistribution of mafic phases and, possibly, sulfides. The Ni/Cr variation for each site appears to reflect at least two converging trends (Fig. 9). This feature represents the ma-

Table 6. Least-squares fractionation solutions, with Zr, Ti, and Sr enrichment factors, for parent–derivative whole-rock pairs.

Parent Sample (interval in cm)	C.T.[a]	Derivative Sample (interval in cm)	C.T.[a]	Olivine (%)	Plagioclase (%)	Clinopyroxene (%)	ΣR^2	$[Zr]_e$	$[Ti]_e$	$[Sr]_e$
482B-22-3, 103–107	D	482B-22-2, 130–136	D	−1.72	−0.90	−2.92	0.08	1.04	1.05	0.97
482D-10-1, 106–109	F	482D-10-2, 70–72	E	−3.43	−12.43	−7.65	0.04	1.37	1.27	1.15
483B-8-1, 55–61	D	483B-8-1, 29–35	D	−1.45	+5.63	−0.62	0.12	0.97	0.96	1.31
483-16-3, 2–6	C	483B-7-3, 2–6	C	−1.36	−1.63	−0.41	0.29	1.03	1.03	0.99
483B-4-1, 26–30	B	483-15-1, 93–97	B	−0.91	+1.71	−0.01	0.15	0.99	0.99	1.20
483-24-2, 35–40	H	483-25-2, 61–66	H	−0.95	+0.72	−0.41	0.01	1.00	1.00	1.01
483B-20-2, 50–59	H	483B-20-2, 16–21	H	−0.51	+5.55	−0.20	0.24	0.96	0.95	1.02
483B-28-3, 37–40	K	483B-27-1, 12–18	K	−3.63	−2.16	−8.55	0.12	1.14	1.13	1.04
483B-29-1, 10–15	K	483B-25-2, 22–28	K	−2.97	−5.52	−10.40	0.10	1.16	1.19	1.13
483B-26-2, 126–137	K	483B-27-1, 114–119	K	−3.81	−1.91	−0.11	0.17	1.03	1.06	1.02
485A-11-3, 68–73	A	485A-11-3, 116–121	A	−3.39	+1.63	−0.39	0.06	1.01	1.02	1.70
485A-11-3, 68–73	A	485A-11-3, 57–60	A	−5.33	+0.31	−8.48	0.01	1.08	1.12	1.68
485A-13-1, 110–117	E	485A-13-1, 11–8	E	−1.29	+2.31	−0.40	0.18	0.99	0.99	0.95
485A-25-1, 117–143	H	—		−2.42	−4.75	−1.65	0.07	1.07	1.09	1.01
485A-32-3, 47–51	I	485A-32-6, 52–57	I	−2.38	−6.17	−2.63	0.08	1.14	1.12	0.99
485A-33-2, 26–33	I	485A-33-2, 88–94	I	−0.96	−0.60	−1.17	0.10	1.10	1.02	1.04
485A-38-3, 18–23	L	485A-38-6, 58–63	L	−2.72	−3.35	−0.14	0.05	1.08	1.07	0.99

Note: ΣR^2 = square of summed residuals; $[\ ]_e$ = enrichment factor (derivative/parent concentration).
[a] C.T. = chemical type

jor distinction between Types B and F at Site 482, which are otherwise indistinguishable (Fig. 3). At Site 483, Types F, H, I, J, K, L, and M (the "lower" massive and pillow flows) together with Type D (from the upper massive flows) correspond to the high Ni/Cr trend, while Types C and B (also from the upper massive flows) belong to the lower Ni/Cr trend. None of the Site 485 types displays a low Ni/Cr ratio, but Type J is intermediate between the two main trends that characterize the other sites. As with other element variation trends, the Ni/Cr pattern for Cooling Unit 10 (Type I) is complex, in contrast to most of the other cooling units at Site 485.

In summary, each chemical type appears to represent an individual fractionation trend superimposed on one or several preexisting "liquid"-type trend(s). Several fractionation "series" consisting of Types F–K, J–K–L, and M–? are tentatively inferred from the Ti/Zr variations at Site 483 and appear to be consistent with the Sr, Ni, and Cr variation as well (Fig. 10). Considered stratigraphically (Fig. 2), these may reflect a cyclic eruptive pattern of massive and pillowed lavas (in that order). As indicated by the Y/Zr variation, these chemical types are distinct from the "upper" massive units (Types B, C, and D) with Type D showing the most obvious difference. We note again the apparent conflict between mass balance requirements for plagioclase accumulation and absence or paucity of plagioclase as a phenocryst phase.

SUMMARY AND DISCUSSION

The major and trace element chemistry of the basalts from these sites reveals complex variation patterns which clearly indicate the influence of several types and hierarchies of petrogenetic processes. Fractional crystallization is obviously an important contributor to the variation observed. However, the diversity of the trends at any given site appears inconsistent with single-stage, closed-system fractionation models (Fig. 10). Mass balance models based on least-squares calculations should not be overemphasized in view of analytical (and other) uncertainties. Contradictions of interpretations based on trace and major elements (e.g., Samples 485A-11-3, 68–73 cm and 116–121 cm, in which an increase in Ni from 208 to 233 appears to correspond to the removal of 3.39% olivine) may result from quantitative rather than qualitative inaccuracies in the solution. In general, the mass balance models for single eruptive units suggest that the compositions of these units are the result of repeated episodes of phenocryst redistribution in magma batches derived from earlier, probably more deep-seated, fractionation episodes. Mass balance requirements for several of the massive units indicate that plagioclase accumulation was accompanied by fractional removal of olivine and clinopyroxene. The petrography of some units is consistent with this interpretation, as reflected by significant phenocryst plagioclase associated with little or no mafic phases. However, plagioclase rarely exceeds 5 modal percent, and in several notable examples, is altogether absent (e.g., Types D, K, and H at Site 483 and Types A and I at Site 485).

The accumulation of plagioclase may occur under static or dynamic conditions. During the rise of the magma, cotectic crystallization of olivine, plagioclase, and clinopyroxene may result in gravitational separation of the mafic phases and plagioclase, the latter being retained in suspension (e.g., Fujii and Kushiro, 1977; Kushiro, 1980). Alternatively, plagioclase may accumulate by flotation in a stable crystallizing magma body, a process that Flower (1980) suggests may be favored by higher pressure fractionation regimes (>ca. 5 kb) in view of the relative increase in liquid tholeiite density (Fujii and Kushiro, 1977). In either case, a magma in which plagioclase is present as a cumulate phase will diverge compositionally from "liquid-line" trends. To explain aphyric magmas with the compositional character of cumulates, a mechanism is required for redissolving phenocryst phases such that a totally fluid magma is erupted at the surface. Such explanations are probably best sought in terms of basaltic phase equilibria. Two critical effects are brought to mind: (1) the effect of variable pressure on the stability of solid phases (polybaric fractionation) (O'Hara, 1968; Presnall et al., 1979; Bender et al., 1978) and (2) superheating resulting from proximity to or hybridization with hot primitive magma (e.g., Goode, 1977; Elthon, 1981).

Possible scenarios combining polybaric fractionation regimes and magma mixing could thus explain the principal characteristics of the basaltic variation observed

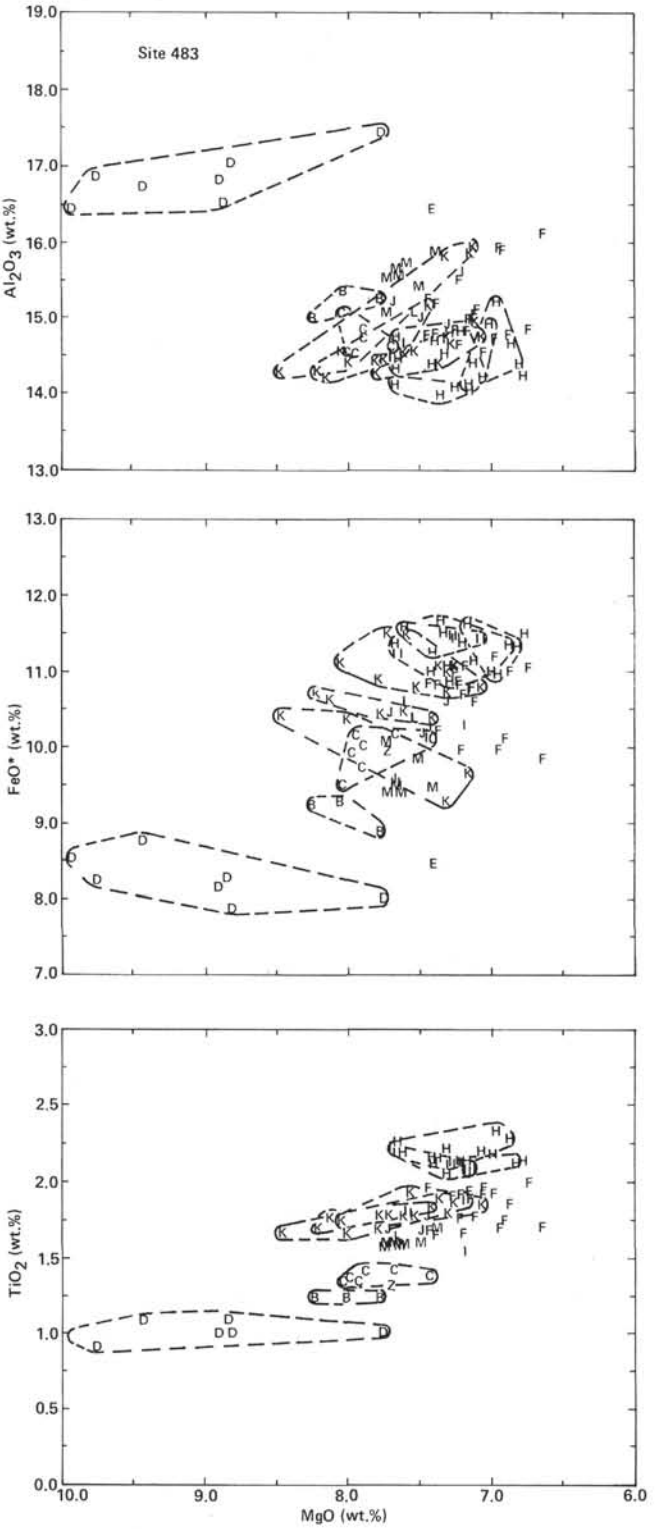

Figure 4. Al_2O_3, FeO*, and TiO_2 versus MgO for Site 483. Dashed lines indicate "upper" and "lower" massive units (Chemical Types B, C, and D and Types H and K, respectively). Pillow lavas consist of Types F, I, J, L, and M; Types B, C, D, and K are aphyric or very sparsely phyric; Type H and pillow basalt sequences are generally more phyric. (Note distinctive massive unit trends compared to overall trends of FeO* and TiO_2-enrichment and Al_2O_3-depletion.)

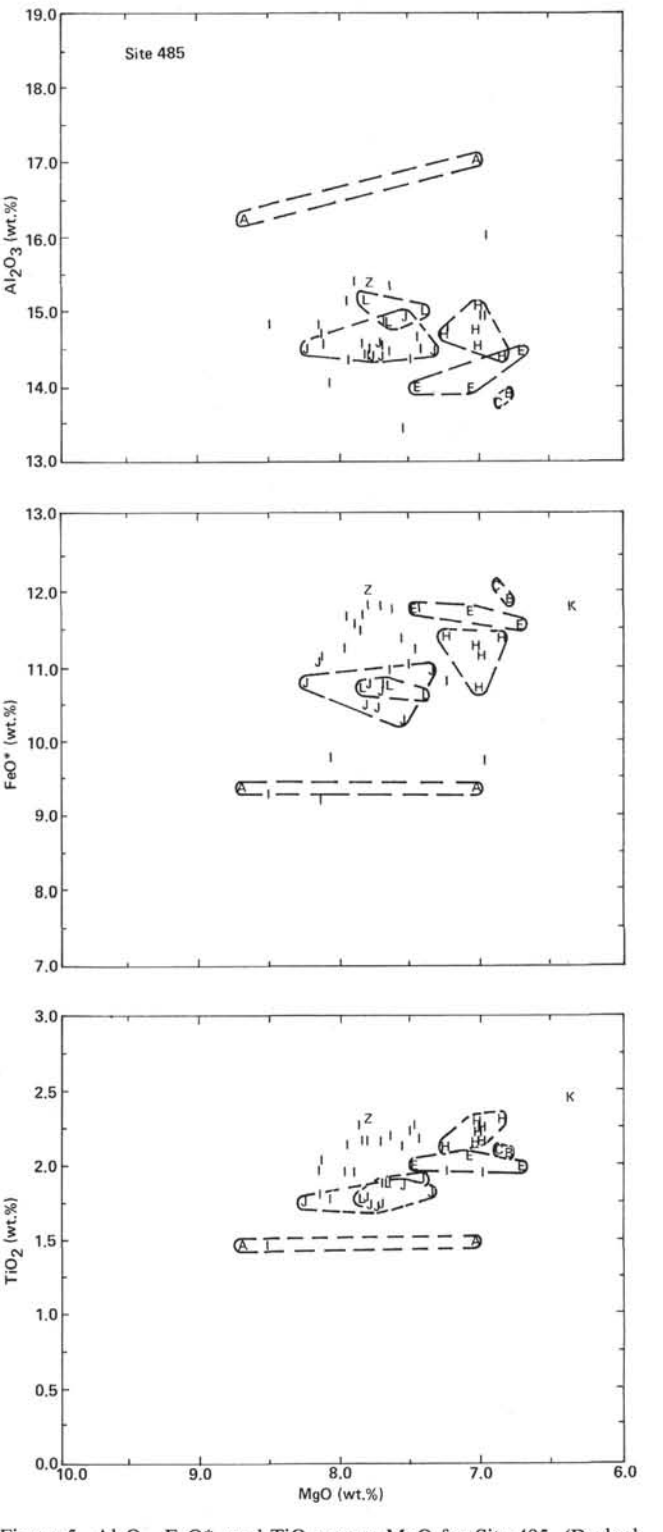

Figure 5. Al_2O_3, FeO*, and TiO_2 versus MgO for Site 485. (Dashed lines indicate chemical types corresponding to lithologic units. Types A, B, and C correspond to Unit 1; Type I corresponds to Unit 5, which is believed to result from multiple eruption and/or intrusion. Note similarity of intra-unit variation to that observed in massive units at Site 483.)

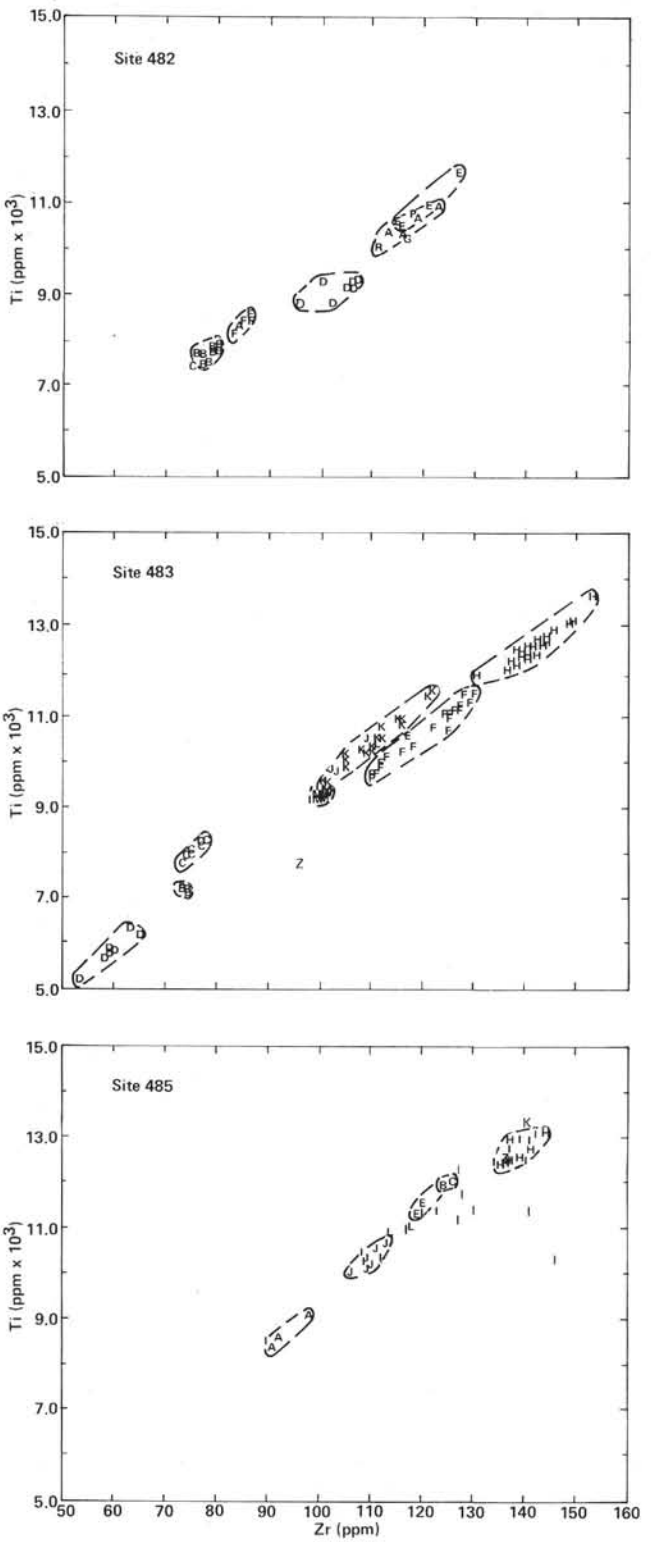

Figure 6. Ti versus Zr for Sites 482, 483, and 485. (Dashed lines indicate chemical types. Note distinctive Ti/Zr ratios for chemical types.)

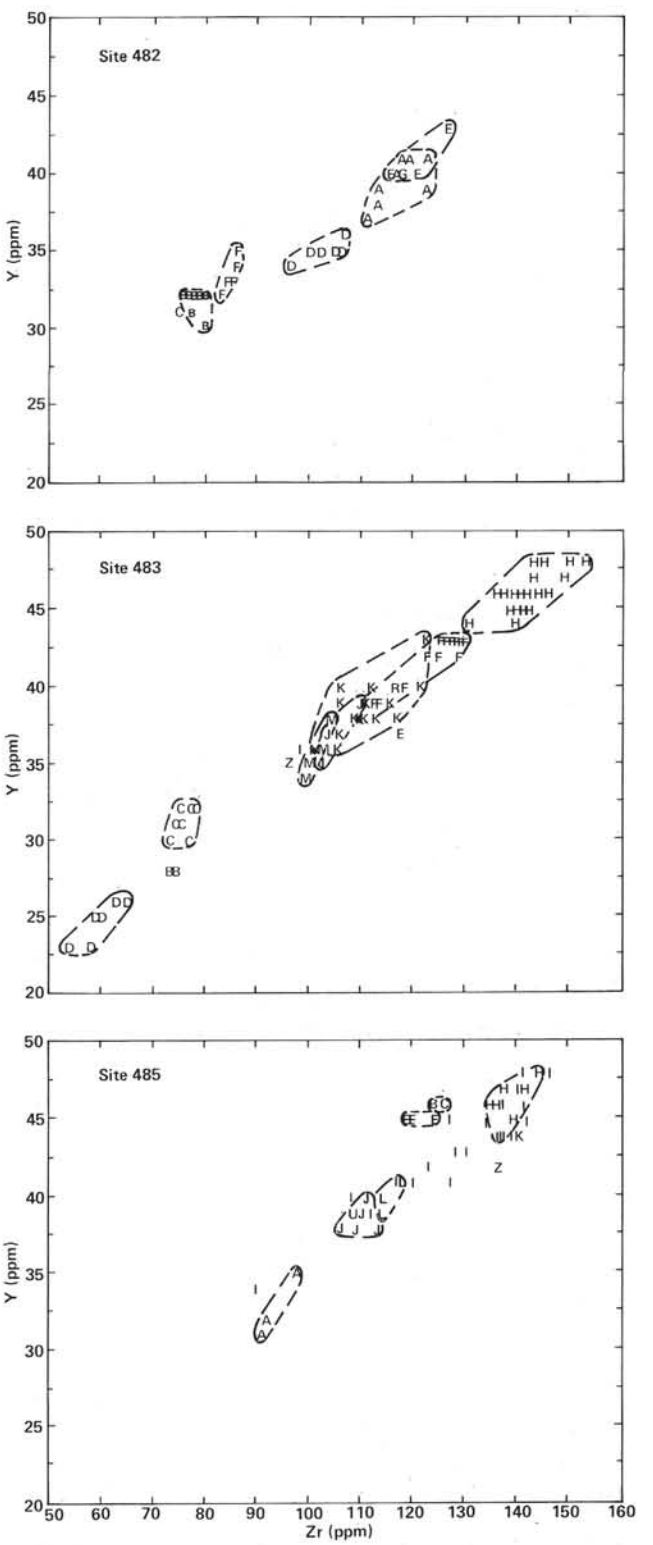

Figure 7. Y versus Zr for Sites 482, 483, and 485. (Dashed lines indicate chemical types. Note approximately continuous between-type variation and the increase in Zr/Y ratio with increasing Zr content.)

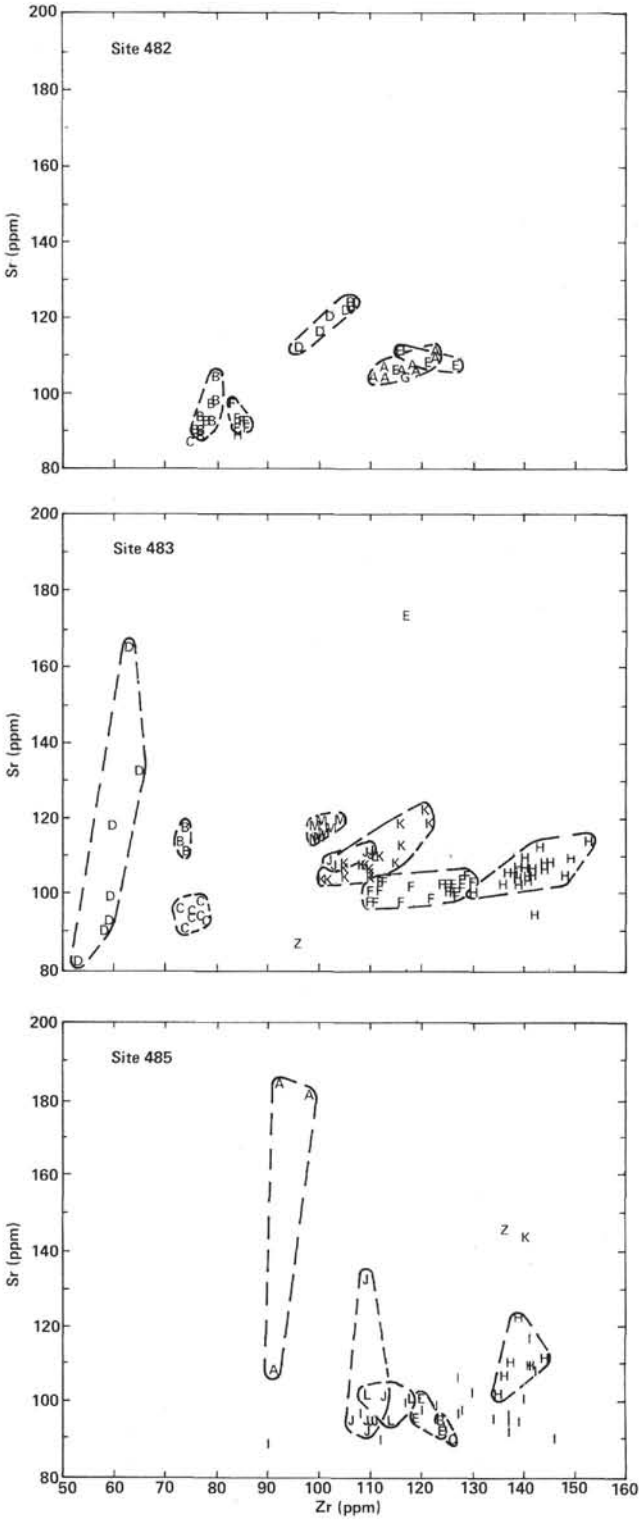

Figure 8. Sr versus Zr for Sites 482, 483, and 485. (Dashed lines indicate chemical types. Note discrepancy between intraunit and overall variation trends [cf. major elements, especially Al_2O_3]. This results partly from plagioclase accumulation.)

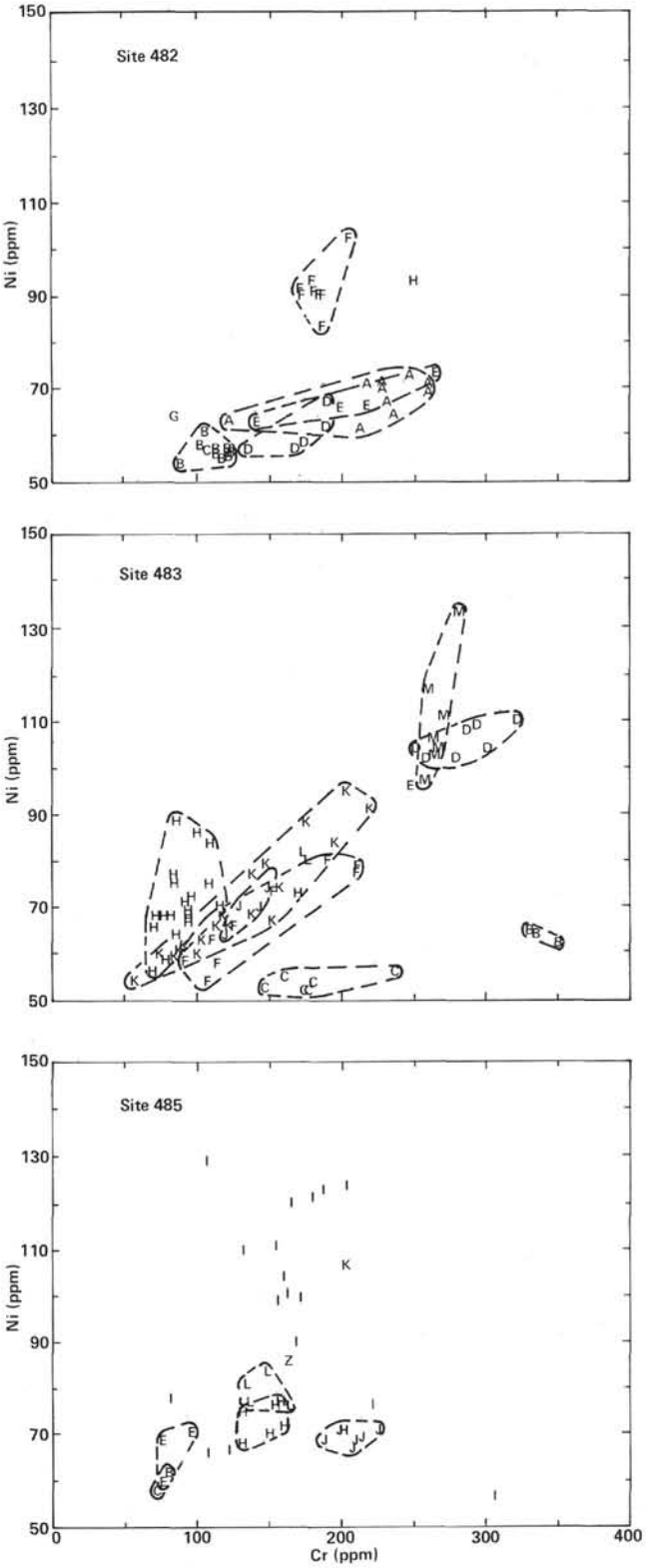

Figure 9. Ni versus Cr for Sites 482, 483, and 485. (Dashed lines indicate chemical types. Note high and low Ni/Cr trends at Sites 482 and 483 and the dispersion of values for Site 485 Type I.)

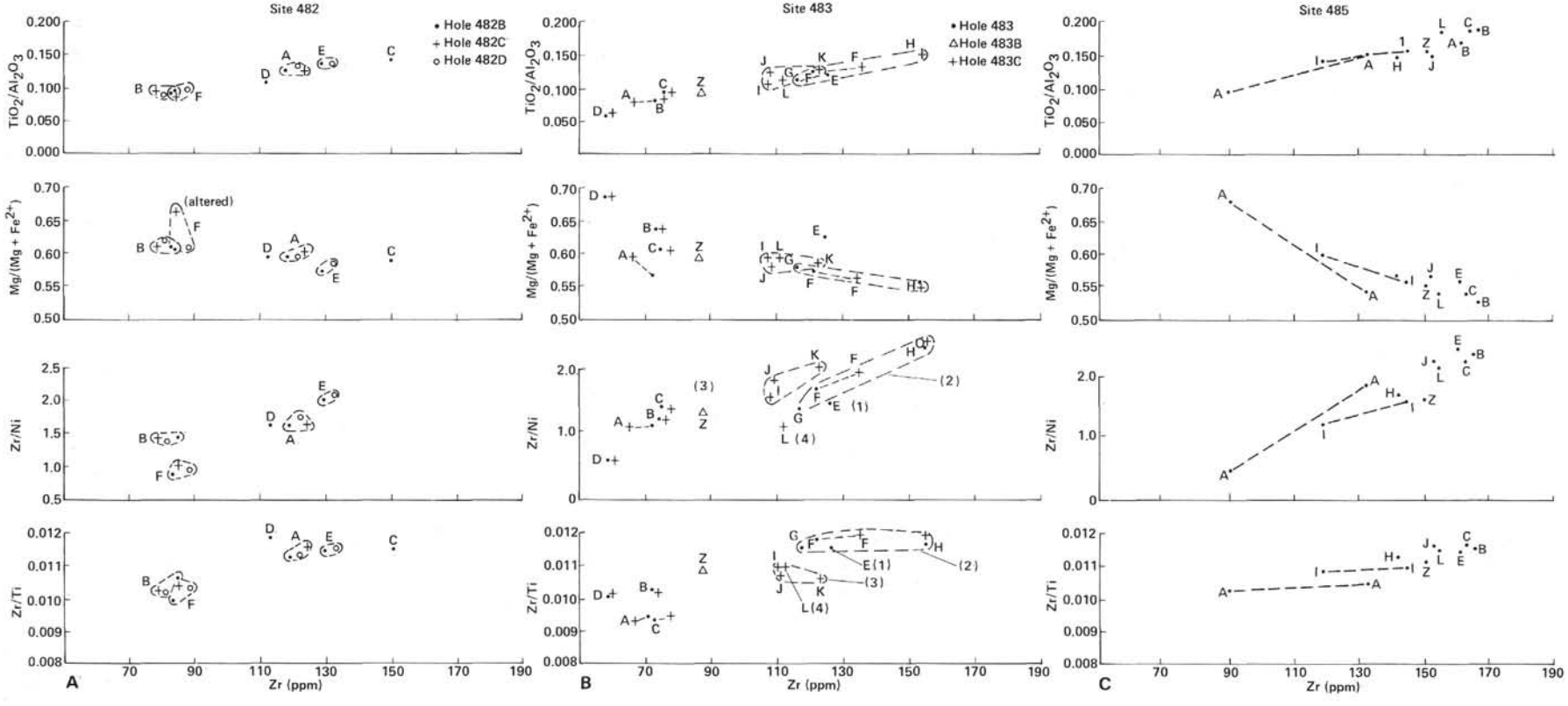

Figure 10. A. Chemical type averages for TiO_2/Al_2O_3, $Mg/(Mg + Fe^{2+})$, Zr/Ni, and Zr/Ti versus Zr for holes at Site 482. B. Chemical type averages for TiO_2/Al_2O_3, $Mg/(Mg + Fe^{2+})$, Zr/Ni, and Zr/Ti versus Zr for holes at Site 483. (Dashed lines indicate massive/pillow unit cyclic sequences.) C. Chemical type averages for TiO_2/Al_2O_3, $Mg/(Mg + Fe^{2+})$, Zr/Ni, and Zr/Ti versus Zr for Site 485. Averages based on composite data sets (this work and shipboard data). (A....A′ and I....I′ indicate low and high MgO subtype averages.)

along this part of the East Pacific Rise. It is noted that the plagioclase-cumulate trends observed in the Leg 65 basalts (cryptic or otherwise) are considerably less well developed than those commonly observed in Atlantic basalts (e.g., from Sites 332, 395, 396, 417, and 418) where, in most cases, plagioclase-enrichment trends are marked by strongly plagioclase-phyric lithologies (Flower, 1980). It should also be noted that the variation patterns shown in Figures 3–9 suggest that mixing was not of the "open-system" type (e.g., O'Hara, 1977; 1981), but occurred, together with fractional crystallization and phenocryst accumulation, during discrete episodes.

In general, the geometric and temporal character of magmatic accretion processes in the southern Gulf of California appears to be intermediate between the processes observed along superfast sections of the East Pacific Rise and those along the slow-spreading Mid-Atlantic Ridge. The magma fractionation systems beneath the Gulf of California axis resemble those of the Mid-Atlantic Ridge in being transient, possibly polybaric and giving rise to plagioclase-cumulate magmas. In contrast, the emplacement of magma appears to be under relatively stable tectonic conditions more typical of the fast-spreading environment.

ACKNOWLEDGMENTS

Thanks are extended to the captain and crew of the D/V *Glomar Challenger* and to the staff of the Deep Sea Drilling Project for ensuring the success of Leg 65. Funding of this research was provided by Deutsche Forschungsgemeinschaft (West Germany), the Smithsonian Institution (Washington, D.C.), the National Research Council (Canada), and the Natural Environment Research Council (U.K.)

REFERENCES

Bender, J. F., Hodges, F. N., and Bence, A. E., 1978. Petrogenesis of basalts from the project FAMOUS area: Experimental study from 0 to 15 kilobars. *Earth Planet. Sci. Lett.*, 41:277–302.

Bryan, W. B., Thompson, G., and Frey, F. A., 1979. Petrologic character of the Atlantic crust from DSDP and IPOD drill sites. *In* Talwani, M., Harrison, C. G., and Hayes, D. E. (Eds.), *Sec. Maurice Ewing Series:* Washington (Am. Geophys. Union), Spec. Publ. 1:237–284.

Byerly, G. R., and Wright, T. L., 1978. Origin of major element chemical trends in DSDP Leg 37 basalts, Mid-Atlantic Ridge. *J. Volcanol. Geotherm. Res.*, 3:229–279.

CYAMEX Scientific Group, in press. First manned submersible dives on the East Pacific Rise, 21°N. (Project RITA): General results. *Mar. Geophys. Res.*

Elthon, D., 1979. High magnesia liquids as the parental magma for ocean floor basalts. *Nature*, 278:514–518.

_____, 1981. One atmosphere phase equilibria of basalts from the Tortuga ophiolite complex, with implications for magma chamber processes. *The Generation of Oceanic Lithosphere* (Chapman Conference, Airlie House, Virginia), p. 10.

Flower, M. F. J., 1980. Accumulation of calcic plagioclase in ocean-ridge tholeiite: An indication of spreading rate?. *Nature*, 287: 530–532.

_____, 1981. A thermal-kinematic model for ocean-ridge magma fractionation. *J. Geol. Soc. Lond.:* 138.

Flower, M. F. J., and Robinson, P. T., 1978. Evolution of the FAMOUS ocean ridge segment: Evidence from submarine and deep sea drilling investigations. *In* Talwani, M., Harrison, C. G., and Hayes, D. E. (Eds.), *Deep Drilling Results in the Atlantic Ocean: Ocean Crust. Sec. Maurice Ewing Series:* Washington (Am. Geophys. Union), pp. 314–330.

_____, 1981a. Basement drilling in the Western Atlantic. 1. Magma fractionation and its relation to eruptive chronology. *J. Geophys. Res.*, 86:6273–6298.

_____, 1981b. Basement drilling in the Western Atlantic. 2. A synthesis of construction processes at the Cretaceous ridge axis. *J. Geophys. Res.*, 86:6299–6309.

Flower, M. F. J., Robinson, P. T., Ohnmacht, W., Marriner, G., and Schmincke, H.-U., 1980. Lithologic and chemical stratigraphy at DSDP Sites 417 and 418. *In* Donnelly, T., Francheteau, J., Bryan, W., Robinson, P., Flower, M., Salisbury, M., et al., *Init. Repts. DSDP*, 51, 52, 53, Pt. 2: Washington (U.S. Govt. Printing Office), 939–956.

Flower, M. F. J., Robinson, P. T.,, Schmincke, H.-U., and Ohnmacht, W., 1977. Magma fractionation systems beneath the Mid-Atlantic Ridge near 36–37°N. *Contr. Mineral. Petrol.*, 64:167–195.

Fujii, T., and Kushiro, I., 1977. Density, viscosity and compressibility of basaltic liquid at high pressure. *Dir. Geophys. Lab., Carnegie Inst. Washington Yearbook*, 76:419–424.

Francheteau, J., Juteau, T., and Rangin, C., 1979. Basaltic pillars in collapsed lava-pools on the deep ocean floor. *Nature*, 281: 209–211.

Goode, A. D. T., 1977. Flotation and remelting of plagioclase in the Kalka Intrusion, central Australia: Petrological implications for anorthosite genesis. *Earth Planet. Sci. Lett.*, 34:379–397.

Huppert, H. E., and Sparks, R. S. J., 1980. Restrictions on the compositions of mid-ocean ridge basalts: A fluid dynamical investigation. *Nature*, 286:46–48.

Kastens, K. A., Macdonald, K. C., Becker, K., and Crane, K., 1979. The Tamayo transform fault in the mouth of the Gulf of California. *Mar. Geophys. Rev*, 4:129–131.

Kushiro, I., 1980. Viscosity, density, and structure of silicate melts at high pressures, and their petrological applications. *In* Hargraves, R. B. (Ed.), *Physics of Magmatic Processes:* Princeton (Princeton University Press), pp. 93–120.

Lewis, B. T. R., 1979. Periodicities in volcanism and longitudinal magma flow on the East Pacific Rise at 23°N, *Geophys. Res. Lett.*, 6:53–756.

O'Hara, M. J., 1968. The bearing of phase equilibrium studies in synthetic and natural systems on the origin and evolution of basic and ultrabasic rocks. *Earth Sci. Rev.*, 4:69–133.

_____, 1977. Geochemical evolution during fractional crystallization of a periodically refilled magma chamber. *Nature*, 266: 503–507.

_____, 1981 Geochemical evolution in an advancing, periodically replenished, periodically tapped, continuously fractionated magma chamber. *J. Geol. Soc. Lond.*, 138.

Presnall, D. C., Dixon, J. G., O'Donnell, T., and Dixon, S. A., 1979. Generation of mid-ocean ridge tholeiite. *J. Petrol.*, 20:3-35.

Reid, I., Orcutt, J. A., and Prothero, W. A., 1977. Seismic evidence for a narrow zone of partial melting underlying the East Pacific Rise at 21°N. *Bull. Geol. Soc. Am.*, 88:678–682.

APPENDIX A
Analyzed Whole-Rock Samples

Sample (interval in cm)	Lithologic Unit	Cooling Unit	Chemical Type
Hole 482B			
13-1, 99–104	1	1 (massive)	A
14-1, 91–94		5 (massive)	F
14-1, 132–137		6	F
14-3, 2–6		8 (massive)	F
14-4, 16–20		8	F
15-1, 12–16		9 (massive)	F
16-4, 100–104	2	11 (massive)	B
20-1, 27–30	4	13 (massive)	B
20-3, 144–147	6	15 (massive)	D
21-2, 19–23		15	D
21-3, 58–63	7	16 (massive)	D
22-2, 67–72		16	D
22-2, 130–136		16	D
22-3, 103–107		16	D

Appendix A. (Continued).

Sample (interval in cm)	Lithologic Unit	Cooling Unit	Chemical Type
Hole 482B			
22-4, 97–102		16	D
24-3, 110–115	8	17 (massive)	D
Hole 482C			
10-1, 0–4	1	1 (massive)	A
10-1, 9–12		1	A
10-1, 12–16		1	A
10-3, 11–14		1	A
11-3, 65–69		2 (massive)	A
12-1, 92–118	2	3 (massive)	B
13-1, 10–15		4 (massive)	B
14-1, 13–18		5 (massive)	B
15-1, 114–118		7 (massive)	B
Hole 482D			
8-1, 24–29	1	1 (massive)	A
8-1, 65–72		1	A
10-1, 106–109	2	3 (massive)	F
10-1, 111–114		3a	E
10-2, 70–72		3a	E
10-2, 128–130		3a	E
10-3, 25–27		3a	E
10-3, 93–97	3	5 (pillow?)	F
12-1, 28–32		10 (pillow?)	F
12-3, 27–31	4	12 (massive)	B
13-1, 49–51		14 (massive)	B
13-1, 98–101		14	B
13-1, 128–134		14	B
Hole 482F			
5-1, 133–139	1	1 (massive)	G
11-1, 125–128		1(?)	H
Hole 483			
14-1, 58–68	2	2a (massive)	B
15-1, 93–97		2b	B
16-2, 64–70	3	3 (massive)	C
16-2, 99–100		3	C
16-3, 2–6		3	C
17-2, 13–17	4	4 (massive)	D
17-2, 17–21		4	D
18-4, 131–134	5	5 (massive)	E
21-1, 49–55	6	13 (pillow)	F
21-1, 57–61		13	F
21-3, 6–9		16 (pillow)	F
22-2, 68–72		23 (pillow)	F
22-2, 74–77		23	F
22-2, 85–88		23	F
22-2, 88–93		23	F
22-2, 94–99		23	F
23-1, 10–16		36 (pillow)	F
24-1, 52–57	7 (a)	40 (massive)	H
24-2, 35–40		41 (massive)	H
25-2, 61–66		44 (massive)	H
26-1, 59–63	7 (b)	45 (massive)	H
26-2, 40–44		46 (massive)	H
26-3, 124–130		46	H
Hole 483B			
4-1, 26–30	2	2 (massive)	B
7-1, 7–12	3	3 (massive)	C
7-1, 26–31		3	C
7-2, 56–61		3	C
7-3, 2–6		3	C

Appendix A. (Continued).

Sample (interval in cm)	Lithologic Unit	Cooling Unit	Chemical Type
Hole 482B (Cont.)			
8-1, 29–35	4	4 (massive)	D
8-1, 55–61		4	D
8-1, 120–126		4	D
8-2, 121–126		4	D
8-7, 2–20		4	D
12-1, 92–95	5(a)	8 (pillow)	I
13-1, 38–44	5(b)	12/23 (pillow)	F
13-1, 60–64		12/23	F
13-1, 60–64		12/23	F
13-1, 66–67		13/24 (pillow)	F
13-1, 66–67		13/24 (pillow)	F
13-1, 74–79		13/24	F
13-1, 92–98		13/24	F
13-1, 108–119		13/24	F
13-1, 115–122		13/24	F
13-1, 115–122		13/24	F
13-1, 124–131		14/25 (pillow)	F
13-1, 124–131		14/25	F
13-1, 134–139		14/25	F
14-1, 130–133		21/32 (pillow)	F
18-1, 49–52	6(b)	24/40 (massive)	H
18-1, 103–107		24/40	H
18-2, 18–22		24/40	H
19-2, 17–21	6(c)	25/42 (massive)	H
19-2, 104–108	6(d)	26/43 (massive)	H
19-3, 8–12		26/43	H
20-1, 14–19		26/44	H
20-1, 94–99		26/44	H
20-2, 9–14		26/44	H
20-2, 16–21		26/44	H
20-2, 25–30		26/44	H
20-2, 37–42		26/44	H
20-2, 50–59		26/44	H
20-2, 50–59		26/44	H
20-2, 50–59		26/44	H
20-2, 142–146	7(a)	27/46 (massive)	H
21-2, 57–61	7(b)	31/50 (pillow)	J
22-1, 26–32		35/54 (pillow)	J
22-2, 63–67		39/58 (pillow)	J
22-2, 77–82		39/58 (pillow)	J
23-4, 19–24		49/68 (pillow)	J
25-2, 18–20	8(a)	57/77 (massive)	K
25-2, 22–28		58/78 (massive)	K
25-2, 39–45		58/78	K
26-2, 42–47		58/80	K
26-2, 126–137		58/81	K
27-1, 12–18	8(b)	59/83 (massive)	K
27-1, 114–119		59/83	K
27-2, 95–101		59/83	K
27-3, 94–98		59/83	K
27-4, 74–80		59/83	K
28-1, 42–59	8(c)	60/84 (massive)	K
28-1, 123–128		60/84	K
28-2, 28–32		60/84	K
28-3, 37–40		60/84	K
29-1, 10–15		60/85	K
29-1, 26–31		60/85	K
29-1, 40–45		60/85	K
29-1, 55–57		60/85	K
29-1, 57–62		60/85	K
29-1, 57–62		60/85	K
30-3, 13–16	9	68/94 (pillow)	L
30-3, 18–22		69/95 (pillow)	L
31-3, 20–25		74/101 (pillow)	M
32-1, 1–6		77/104 (pillow)	M
32-1, 27–31		77/104	M
32-1, 44–50		77/104	M

Appendix A. (Continued).

Sample (interval in cm)	Lithologic Unit	Cooling Unit	Chemical Type
Hole 482B (Cont.)			
32-1, 90–94		77/104	M
32-1, 90–94		77/104	M
32-1, 84–88		77/104	M
Hole 483C			
4-4, 58–66	1	1 (massive)	Z
Hole 485A			
11-3, 57–60	1	1/1 (massive)	A
11-3, 68–73		1/1	A
11-3, 116–121		1/1	A
12-1, 10–16		2/3 (massive)	B
12-1, 76–82		3/4 (massive)	C
12-1, 114–120		5/6 (massive)	E
13-1, 11–18		5/7	E
13-1, 110–117		5/7	E
17-1, 77–82	2	6(?)	Z
23-1, 50–56	4	8/12 (pillow?)	H
23-1, 50–56		8/12	H
23-2, 16–22		8/12	H
23-3, 120–125		8/12	H
25-1, 117–143		8/14	H
29-1, 2–8	5	9/16 (massive)	I
29-1, 89–93		9/16	I
29-2, 143–148		9/16	I
29-3, 10–16		9/16	I
30-2, 96–101		9/19	I

Appendix A. (Continued).

Sample (interval in cm)	Lithologic Unit	Cooling Unit	Chemical Type
Hole 485A (Cont.)			
30-3, 38–41		9/19	I
30-3, 44–49		9/19	I
30-4, 8–13		9/19	I
31-1, 62–67		9/20	I
31-3, 34–39		9/20	I
32-1, 55–61		9/20	I
32-2, 99–105		9/21	I
32-3, 47–51		9/21	I
32-5, 9–14		9/21	I
32-6, 52–57		9/21	I
33-1, 2–9		9/22	I
33-1, 74–79		9/22	I
33-2, 26–33		9/22	I
33-2, 72–78		9/22	I
33-2, 88–94		9/22	I
34-1, 86–90	6	10/23 (massive)	J
34-2, 96–102		10/23	J
35-1, 135–142		10/23	J
35-2, 113–118		10/24	J
35-3, 21–27		10/24	J
35-4, 85–92		10/24	J
35-6, 47–53		10/24	J
36-3, 65–69	7	11/25 (massive)	K
38-3, 18–23	8	12/27 (massive)	L
38-6, 58–63		12/27	L
39-1, 26–32		12/28	L
39-1, 59–64		12/28	L

APPENDIX B
Correlation of Lithologic and Cooling Units with Chemical Types, Sites 482, 483, and 485

Lithologic Unit	Top (m)[a]	Base (m)[a]	Cooling Units	Phenocryst Assemblage	Core-Section (level in cm)	Chemical Type
Hole 482B						
1	136.5	158.0	1–4	Aphyric	10-7, 8 to 15-1, 115	A, F
2	158.0	174.7	10–11	Plagioclase	15-1, 115 to 17-2, 150	B
Sedimentary intercalation						
3	184.1	186.2	12	Plagioclase	18-1, 90 to 18-2, 107	B
4	193.5	199.5	13	Plagioclase	19-1, 60 to 20-2, 83	C
5	199.5	201.5	14	Plagioclase-Clinopyroxene	20-2, 83 to 20-3, 130	D
6	201.5	205.0	15	Plagioclase-Clinopyroxene-Olivine	20-3, 130 to 21-3, 50	E
7	205.0	220.3	16	Plagioclase-Clinopyroxene-Olivine	21-3, 50 to 23-1, 30	D
Sedimentary intercalation						
8	224.7	229.0	17	Aphyric	24-1, 25 to 24-3,130	D
Hole 482C						
1	135.5	157.0	1–2	Aphyric	9-1, 60 to 12-1, 0	A
2	157.0	184.0	3–7	Plagioclase-Clinopyroxene-Olivine	12-1, 0 to 15-4, 145	F, B
Hole 482D						
1	138.0	139.6	1–2	Aphyric	8-1, 0 to 8-2, 30	A
Sedimentary intercalation						
2	141.7	154.0	3	Aphyric	9-1, 15 to 10-3, 60	F, E
Sedimentary intercalation						
3	154.1	169.6	4–10	Aphyric	10-3, 65 to 12-1, 130	F
4	169.6	186.5	11–16	Plagioclase	12-1, 130 to 13-3, 35	B
Hole 483						
1	110.0	111.0	1	Plagioclase-Olivine	13-4, 5 to 13-4, 95	A
Sedimentary intercalation						
2	115.0	127.0	2(a-b)	Aphyric	14-1, 5 to 15-2, 128	B
Sedimentary intercalation						
3	127.0	135.8	3	Aphyric	15-2, 128 to 16-3, 12	C
Sedimentary intercalation						
4	142.2	145.0	4	Aphyric	17-1, 18 to 17-3, 24	D
Sedimentary intercalation						
5	156.5	160.1	5	Aphyric	18-4, 130 to 19-1, 10	E
Sedimentary intercalation						
6a		(171.0)			unrecovered	F?
Sedimentary intercalation						
6b	169.0	186.5	6–27	Plagioclase-Olivine-Clinopyroxene	20-1, 5 to 22-4, 60	F
6c	186.5	188.5	28	Plagioclase-Olivine	22-4, 60 to 23-2, 20	F-X
6d	188.5	190.0	29–30	Plagioclase-Olivine-Clinopyroxene	23-2, 20 to 23-2, 150	F

Appendix B. (Continued).

Lithologic Unit	Top (m)[a]	Base (m)[a]	Cooling Units	Phenocryst Assemblage	Core-Section (level in cm)	Chemical Type
Sedimentary intercalation						
7a	191.5	200.3	31–34	Plagioclase-Olivine	24-1, 5 to 26-1, 40	H
Sedimentary intercalation						
7b	200.4	204.5	35	Plagioclase	26-1, 50 to 26-3, 150	H
Hole 483B						
1	110.0	111.3	1	Plagioclase-Olivine	2-7, 0 to 3-1, 75	A
Sedimentary intercalation						
2	111.3	127.0	2	Aphyric	3-1, 75 to 4-7, 20	B
Sedimentary intercalation						
3	133.0	136.4	3	Aphyric	7-1, 7 to 7-3, 75	C
Sedimentary intercalation						
4	137.6	146.8	4	Aphyric	8-1, 10 to 9-1, 44	D
Sedimentary intercalation						
5a	169.0	175.0	6–10	Plagioclase-Olivine-Clinopyroxene	12-1, 0 to 13-1, 10	I
5b	175.0	184.6	11–22	Plagioclase-Olivine-Clinopyroxene	13-1, 10 to 15-1, 6	F
Sedimentary intercalation						
6a	194.0	197.3	23	Aphyric	17-1, 0 to 17-3, 45	H
Sedimentary intercalation						
6b	199.0	204.6	24	Aphyric	18-1, 0 to 19-1, 65	H
Sedimentary intercalation						
6c	204.6	206.2	25	Aphyric	19-1, 65 to 19-2, 85	H
6d	206.2	210.5	26	Plagioclase-Olivine-Clinopyroxene	19-2, 85 to 20-2, 65	H
Sedimentary intercalation						
7a	211.1	213.0	27	Plagioclase-Olivine	20-2, 130 to 20-3, 30	H?
7b	213.0	227.7	28–56	Plagioclase-Clinopyroxene-Olivine	21-1, 0 to 24-1, 145	J
Sedimentary intercalation						
8a	227.7	232.4	57	Plagioclase-Clinopyroxene-Olivine	24-1, 145 to 25-2, 5	K
Sedimentary intercalation						
8b	232.6	236.9	58	Plagioclase-Olivine	25-2, 20 to 26-1, 150	K
Sedimentary intercalation						
8c	237.0	249.5	59	Plagioclase-Olivine	26-2, 5 to 29-1, 65	K
Sedimentary intercalation						
9	249.5	267.0	60–82	Plagioclase-Olivine-Clinopyroxene	29-1, 65 to 32-3, 82	L, M
Hole 483C						
1	109.5	114.0	1	Aphyric	4-2, 47 to 4-5, 120	A
485A						
1	153.5	159.4	1–5	Plagioclase-Olivine-Clinopyroxene	11-3, 55 to 13-1, 140	A–E
Sedimentary intercalation						
2	180.5	184.0	?	Plagioclase	17-1, 0 to 18-1, 58	Z
Sedimentary intercalation						
3	201.5	202.0	?	Plagioclase	22-1, 0 to 22-1, 3	?
Sedimentary intercalation						
4	212.0	226.2	8	Plagioclase-Olivine	23-1, 50 to 26-1, 20	H
Sedimentary intercalation						
5	239.5	270.4	9	Plagioclase	29-1, 0 to 33-2, 95	I
Sedimentary intercalation						
6	277.5	294.0	10	Plagioclase-Olivine	34-1, 56 to 35-6, 55	J
Sedimentary intercalation						
7	298.6	298.7	11	Plagioclase	36-3, 64 to 36-cc,31	K
Sedimentary intercalation						
8	314.5	328.5	12	Plagioclase	38-2, 2 to 39-5, 60	L

[a] Calculated from core log and corrected for spacers.